EFFECTS OF MOORING CONFIGURATION ON HYDRAULIC PERFORMANCE OF THE H-TYPE FLOATING BREAKWATER (H-FLOAT) IN REGULAR AND RANDOM WAVES

by

MOHAMAD SAFWAN SYAHIR BIN MOHD AZMI

13548

Supervisor: Dr. Teh Hee Min

Civil Engineering Department

Effects of Mooring Configuration on Hydraulic Performance of the H-Type Floating Breakwater (H-Float) in Regular and Random Waves

by

Mohamad Safwan Syahir Bin Mohd Azmi

13548

Dissertation submitted in partial fulfillment of
the requirements for the
Bachelor of Engineering (Hons)
(Civil Engineering)

MAY 2014

Universiti Teknologi PETRONAS
Bandar Seri Iskandar
31750 Tronoh
Perak Darul Ridzuan

CERTIFICATION OF APPROVAL

Effects of Mooring Configuration on Hydraulic Performance of the H-Type Floating Breakwater (H-Float) in Regular and Random Waves

By

Mohamad Safwan Syahir Bin Mohd Azmi

13548

A project dissertation submitted to the
Civil Engineering Department
of Universiti Teknologi PETRONAS
in partial fulfillment of the requirement for the
BACHELOR OF ENGINEERING (Hons)
(CIVIL ENGINEERING)

Approved by,

_____

(Dr. Teh Hee Min)

UNIVERSITI TEKNOLOGI PETRONAS
TRONOH, PERAK
May 2014

CERTIFICATION OF ORIGINALITY

This is to certify that I am responsible for the work submitted in this project, that the original work is my own except as specified in the references and acknowledgements, and that the original work contained herein have not been undertaken or done by unspecified sources or persons.

Safwan Syahir

_____

MOHAMAD SAFWAN SYAHIR BIN MOHD AZMI

ABSTRACT

This study is focuses on the hydraulic investigation of the H-Type floating breakwater (H-Float) which is assessed by physical modelling. The objective of this study is to evaluate the hydraulic performance of the H-Float in both regular and random waves. This study also is aim to ascertain the hydraulic characteristics of H-Float with respect to mooring systems used which are taut leg and catenary. At the end of the study, the hydraulic performance of the H-Float will be compared with other floating breakwater. During the past studies of this H-Float, small number of tests were conducted due to budget and time constraints. The tests conducted were confined to limited test ranges such as wave period, breakwater draft and also water depth. To tackle this issues, thorough study has been carried out on the related subjects and also the development of the previous floating breakwater. The H-Float model also is modified to improve its performance as compared to the past tests done before. The model with a scale of 1:15 is tested in the modified wave tank with a total of 84 tests altogether, subjected to regular and random waves. Other equipment that are used in the test are wave generators, wave probes and wave absorbers. The variable parameters for this study include wave period, wave height and type of mooring system. During the test, this model are moored with taut leg and catenary mooring system, in order to avoid excessive movement experienced due the wave actions. Finally, the performance of the H-Float are assessed based on the transmission and reflection coefficients as well as energy dissipation and these results are compared with the previous test and other floating breakwater studies. Conclusively, the H-Float model with scale of 1:15 moored by taut leg mooring system is an effective floating breakwater with an excellent capability in attenuating wave energy, good anti-reflection structure and an outstanding energy dissipater.

ACKNOWLEDGEMENT

The author would like to express his sincere gratitude to Allah S.W.T for all the strength and chance to be involved in this project. A special appreciation to the supervisor, Dr. Teh Hee Min; lecturer of Civil Engineering Department, Universiti Teknologi PETRONAS for his guidance throughout this project. Thank you for the continuous supports and motivation.

To my laboratory partner; Mr Mohamad Irwan bin Iskandar and Miss Wan Syazwani bt Wan Zulkifli who have been conducting the experiments together with the author, thank you for helping along the whole duration of the study as well as for the motivational and emotional support.

Special appreciation is given to the postgraduate students; Miss Nur Zaidah, Miss Noor Diyana and Mr Muhammad Syahmi Maarof for their guidance in preparing and conducting of the experiments as well as in analyzing the experimental results.

A heartfelt appreciation is extended to the Offshore Laboratory technicians and staffs, particularly Mr. Meor Asnawan and Mr. Mohd Zaid for their assistance to the author throughout the whole duration of the study. This study would have been a failure without their constant help in solving problems and errors faced by the author during the experiments.

To Universiti Teknologi PETRONAS, thank you for the opportunity given to the author to conduct a research study for this final year project. The author had received an opportune chance in meeting many wonderful people along the way of completing this project.

To my family, thank you for your prayers and moral support. And last but not least, millions of thanks to the lecturers, technicians and friends who have been contributing for this project indirectly.

Thank you.

MOHAMAD SAFWAN SYAHIR BIN MOHD AZMI

Civil Engineering Department

TABLE OF CONTENTS

LIST OF FIGURES

LIST OF TABLES

SYMBOLS

H_i	incident wave height
H_r	reflected wave height
H_t	transmitted wave height
C_r	reflection coefficient
C_t	transmission coefficient
C_l	energy loss coefficient
C_l^2	energy loss
E_i	incident wave energy
E_r	reflected wave energy
E_t	transmitted wave energy
E_l	energy loss
L	wavelength
T	wave period
f	frequency
B	width of breakwater
h	height of breakwater
l	length of breakwater
D	draft of breakwater
d	water depth
B/L	relative breakwater width
H_i/L_p	incident wave steepness
H_i/gT^2	wave steepness parameter
D/d	breakwater draft-to-water depth ratio

CHAPTER 1

INTRODUCTION

1.1 BACKGROUND OF STUDY

Based on the strategic location for residential, recreational, commercial, and industrial activities, coastal areas are considered as one of the high value places. Hence, it is desirable and necessitate for human being to preserve and maintain the coast against the destructive actions of the waves and currents. In order to do that, a few approaches have been taken over the past few decades to reduce the impact of the wave action towards the coastal area. One of it is the breakwater.

Breakwaters are man-made structures that are placed near the coastlines as barriers to protect marine structures, marinas, harbors and shorelines from ocean waves that carry destructive wave energy. The primary function of breakwater is to attenuate waves action to an acceptable level. Breakwaters structure cannot stop all the wave action. However, they can partially transmitted, partially reflected and partially dissipated the incident wave. For this purpose, different types of breakwaters are used around the world.

Kurum (2010) had roughly distinguish fixed breakwater structure into three main type namely conventional (mound), monolithic and composite. Mound type of breakwater is a simple large heap of loose elements, such as quarry stone, gravel or concrete blocks that are stacked into a triangle shape of structure. The other type of fixed breakwater which is monolithic is designed with a cross section in such a way that the structure act as one solid block. Monolithic is used when space is limited and local water depths are relatively large. On the other hand, composite type of breakwater is a combination of the mound and monolithic. It is often built when the water depth of the ocean gets larger. It is no doubt that fixed breakwaters can offer excellent protection for the coastal areas and higher durability in withstanding the destructive waves, however they contribute several drawbacks that may not be

economically and environmentally friendly. Thus, researchers have developed several types of alternative structures to overcome the restrictions that are associated with fixed breakwaters.

Floating breakwaters have been used as one of the alternative way to overcome the destruction of waves towards the coastal areas. This type of breakwater may be defined as a structure that combines the ability to reduce the height of ocean waves which have superiority in terms of environmental friendly, low cost, mobility and flexibility. To compare floating breakwaters with fixed breakwaters, this type of structure offers more advantages. However, they are not as strong as the fixed one. Table 1.1 shows the summarized advantages and disadvantages of both fixed and floating breakwaters.

Table 1.1: Advantages and disadvantages of fixed and floating breakwater

	Fixed Breakwater	**Floating Breakwater**
Advantages	✓ Protection from high and long period waves ✓ Easily repaired ✓ Habitat for aquatic life ✓ Strong structure	✓ Easily moved / arranged ✓ Insensitive to water depth ✓ Low construction cost ✓ Environmental friendly ✓ Low interference with water circulation and fish migration ✓ Appropriate for use in poor soil area
Disadvantages	✓ Semi-permanent structure ✓ Limited to certain water depth ✓ High construction cost ✓ Can trap debris ✓ Poor water circulation behind structure	✓ Ineffective for high and long period wave ✓ High repair cost ✓ Failure in heavy storm

A lot of researches were conducted over the years to investigate and study the best characteristics in producing more reliable design of floating breakwater. Each of the designs was tested and their performances were improved year by year based on the experiment results. The box-type floating breakwater is the most basic design, and has been widely studied which became the basis for the development of the H-type floating breakwater (Teh & Nuzul, 2013) as shown in Figure 1.1. The new design of H-type floating breakwater, also known as H-Float, offer better results in attenuating wave energy when compared to other conventional floating breakwater designs. However, the tests and experiments conducted were limited and further experiments and modifications are required to improve to the performance of the design.

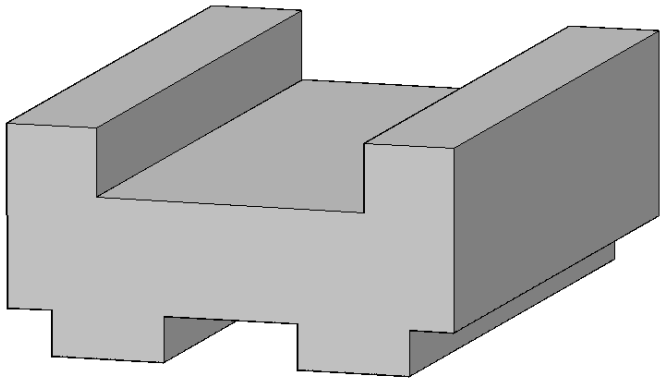

Figure 1.1: H-Type floating breakwater (H-Float) design

1.2 PROBLEM STATEMENT

In the last decade, environmental friendly coastal structures have become one of the great interests in the study of breakwaters. Floating breakwater has been used widely to protect coastal area from destructive ocean wave, especially in the region of deep water depth and soft underground sea, where fixed breakwater is not applicable. A lot of new designs of breakwater are developed each year throughout the studies and experiments. To get the most outstanding results, the ideal experiment is supposed to be carried out in a place with similar setting and condition as the real targeted location. However, due to the time and budget constraint, it is impossible to conduct the experiment and test the capabilities of the floating breakwater out in the open sea. So, all the experiments of the H-type floating breakwater are conducted in

the ocean and coastal laboratory using physical modeling and smaller scales. However, the results of the experiment may be subjected to several drawbacks:

1) Test limitation

   Due to facility and budget constraints, the models were subjected to small test cases such as small range of wave period and limited water depth and breakwater drafts.

2) Inadequate measurement techniques

   The incident and reflected waves were measured by a moving probe method, which were subjected to instrumental and human errors. The limitation on the measuring equipment also might limit the results obtained.

3) Scale effects

   By testing a small-scale test model, it may affect the results compared to the actual size of the breakwater and condition of the wave at the coastal area.

To tackle this problem, several tests will be conducted on the H-type floating breakwater with some modifications that can improve its performance towards some wave conditions.

1.3 OBJECTIVES OF STUDY

The objectives of this study are as follows:

i) To evaluate the hydraulic performances of the H-Float moored by different mooring configuration in both regular and random waves.

ii) To compare the hydraulic performances of the H-Float against other floating breakwaters.

1.4 SCOPE OF STUDY

The scopes of this study are outlined as follows:

1. Literature review

   Thorough studies were carried out on the related subjects and also the development of the previous floating breakwater designs.

2. Model fabrication of the H-Float

   The H-Float is modified with the aim to improve its performance as compared to the previous results of tests done before.

3. Laboratory set-up

   All the test equipment and lab facilities were checked in term of their capabilities, accuracy and precision.

4. Experiments

   Experiments were conducted in a wave tank to assess the hydraulic performance of the H-Float.

5. Analysis of results

   The experimental results obtained from the model were analyzed and compared with other floating breakwaters.

CHAPTER 2

LITERATURE REVIEW

This chapter summarizes general understanding about the parameters used to quantify the amount of wave reflection, wave transmission and energy loss of the floating breakwater. A brief outline on the performance of the other type of floating breakwaters is also included in this study to develop a breakwater design that offer better results in the present study.

2.1 WAVE TRANSMISSION

According to Chakrabarti (1999), the effectiveness of the breakwater in attenuating the wave energy can be determined by the amount of wave energy transmitted beyond the structure. If the transmission coefficient is small, then the breakwater is considered to be effective. It is because, the amount of energy that has transmitted past the structure is much less than the energy of incident wave. The lower the wave transmission coefficient, the higher will be the attenuation of energy.

Wave transmission coefficient C_t can be calculated by using the following formula:

$$C_t = \frac{H_t}{H_i} \tag{2.1}$$

where,

C_t is transmission coefficient

H_t is transmitted wave height (leeward side of the structure)

H_i is the incident wave height (seaward side of the structure)

2.2 WAVE REFLECTION

Chakrabarti (1999) also stated that reflection wave is the re-direction of non-dissipated wave energy by the shoreline or coastal structure to the sea. Reflection occurs when the waves hit on solid seawalls and are reflected back seaward. The reflection coefficient C_r shows the percentage of reflected waves as shown by:

$$C_r = \frac{H_r}{H_i} \tag{2.2}$$

where,

C_r is reflection coefficient

H_r is reflection wave height

H_i is the incident wave height

Total reflection of wave energy will occur without any energy dissipation if the obstruction is a smooth, impermeable and solid vertical structure of infinite height. This would result the *Cr* obtained equal to 1.

2.3 ENERGY LOSS

When a wave hits an obstacle or structure, the wave energy will break down into several parts. The first part of the energy will be reflected back seaward of the structure as reflected wave, while the second part includes the transmitted energy that managed to pass the structure as transmitted wave. The remaining energy is considered as loss energy through the wave dissipation. The energy loss can be calculated by using the following formulas:

$$E_i = E_r + E_t + E_l \tag{2.3}$$

where,

E_i is incident wave energy

E_r is reflected wave energy

E_t is transmitted wave energy

E_l is energy loss

$$E = \frac{(pgH)^2}{8} \tag{2.4}$$

Substituting Eq. (2.4) into Eq. (2.3):

$$\frac{(pgH)^2\ i}{8} = \frac{(pgH)^2\ r}{8} + \frac{(pgH)^2\ t}{8} + \frac{(pgH)^2\ l}{8} \tag{2.5}$$

Simplification:

$$H_i{}^2 = H_r{}^2 + H_t{}^2 + H_l{}^2 \tag{2.6}$$

Dividing Eq. (2.6) by $H_i{}^2$:

$$1 = C_r{}^2 + C_t{}^2 + C_l{}^2 \tag{2.7}$$

where,

C_r is reflection coefficient

C_t is transmission coefficient

C_l is energy loss coefficient

Rearranging Eq. (2.7) will yield:

Energy Loss - $$C_l{}^2 = 1 - (C_t)^2 - (C_r)^2 \tag{2.8}$$

2.4 REGULAR WAVES

Regular waves are monochromatic waves that repeat itself over time in which the vertical displacement of the water surface is the same over a certain period and distance. In other word, regular waves have similar period and amplitude. The vertical displacement of the wave is described as a function of horizontal coordinates *x* and *y*, and time T which is called the period of the waves. The frequency of the waves is $f = \frac{1}{T}$, the angular frequency is $\omega = \frac{2\pi}{T}$, its unit is rad/s. The propagation speed of the waves depends on the period. The waves with the longer period propagate faster than the ones with a smaller period.

The basic example of a regular wave on constant depth (and current velocity) is the sinusoidal wave: $\eta = a\cos(kx - \omega t)$ where a is the amplitude, ω is the angular frequency (as measured at a fixed location in space), and k is the wave number ($k = \frac{2\pi}{\lambda}$ where λ is the wavelength).

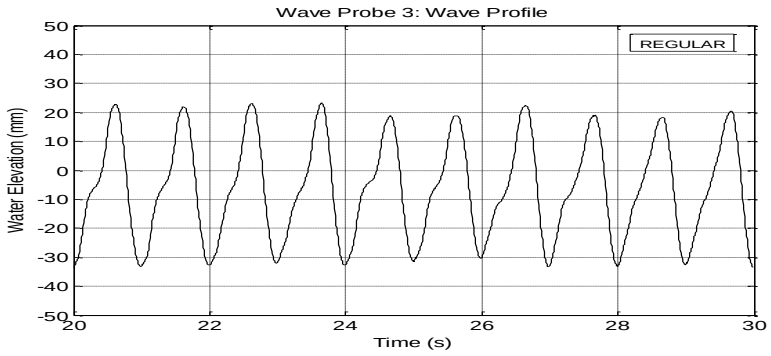

Figure 2.1: Regular wave train

2.5 RANDOM WAVES

Random waves are made up of a large number of regular wave waves of different periods and heights. Random waves do not have a constant wavelength, constant water level elevation but instead it has a random wave phase. When the waves are recorded, a non-repeating wave profile can be seen and the wave surface recorded will be irregular and random. From the profile, some of the individual waves can be identified but overall, the wave profile will show significant changes in height

and period from wave to wave as shown in Figure 2.2. The spectral method and the wave-by-wave analysis are used to study random waves. Spectral approaches are based on Fourier Transform of the water waves. In wave-by-wave analysis, historic periods of water waves are used and statistical records are developed.

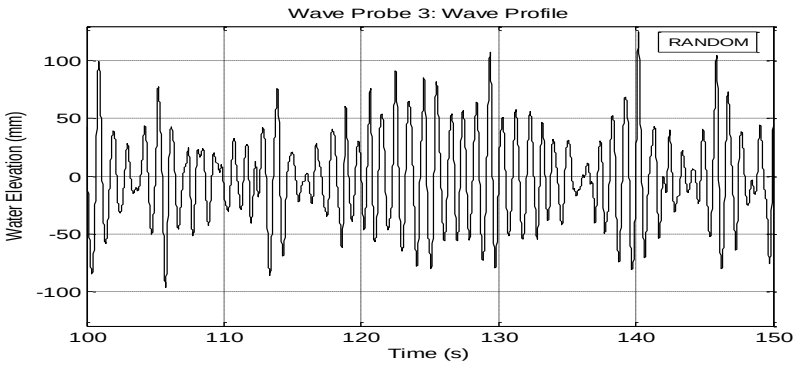

Figure 2.2: Random wave train

2.6 CLASSIFICATION AND PERFORMANCE OF EXISTING FLOATING BREAKWATER

A number of floating breakwaters have been developed and tested by different researchers in the past decades. Hales (1981) reviewed five concepts of floating breakwater which includes the pontoon, sloping floats, scrap tires, cylinders, and tethered float. He suggested that the designs of floating breakwaters should be kept as simple, durable and maintenance free as possible for long time operation in real seas; avoiding highly complex structures that are difficult and expensive to design, construct and maintain.

Later on, McCartney (1985) introduced four types of floating breakwater including box, pontoon, mat, and tethered float. Some examples of the floating breakwater that have been developed and tested as shown in Figure 2.3, will be discussed in this section as follows.

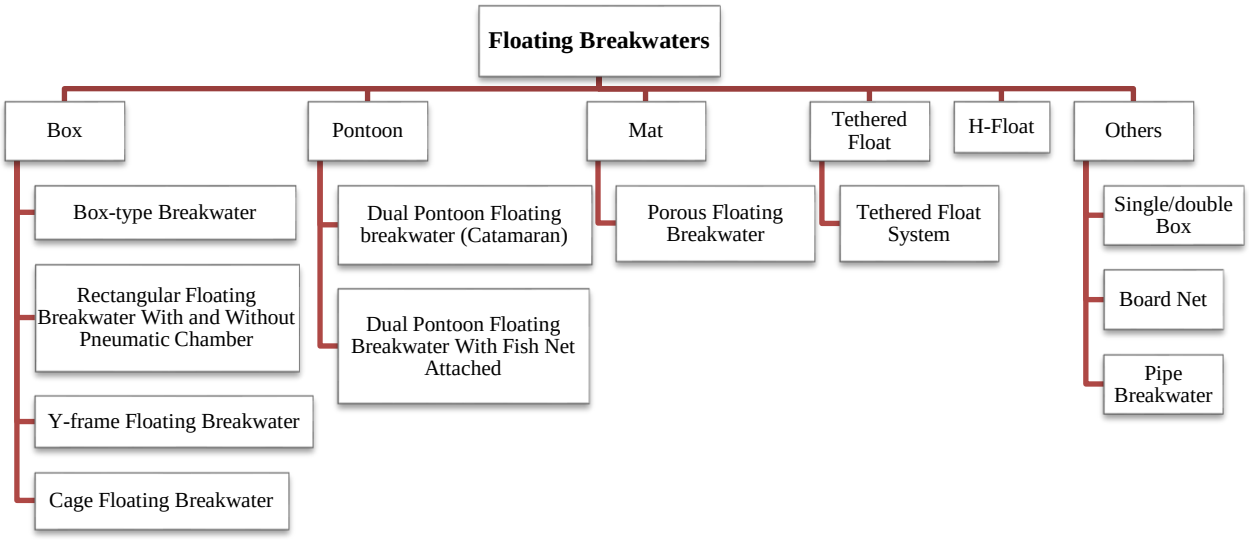

Figure 2.3: Various type of floating breakwater

2.6.1 Box Type Floating Breakwater

McCartney (1985) introduced the box floating breakwater which was constructed of reinforced concrete module. It could be of barge shape or rectangular shape as shown in Figure 2.4. The modules either have flexible connections or are pre-tensioned or post-tensioned to make them act as a single unit. The advantages of the box-type breakwater are it has 50 years design life. Its structure allows pedestrian access for fishing and temporary boat moorage. The shape of the box breakwater is simple to build but a high quality control is needed. It is effective in moderate wave climate. However, the cost of constructing the box type breakwater is very high.

Figure 2.4: Solid rectangular box-type floating breakwater (McCartney, 1985)

2.6.2 Rectangular Floating Breakwater With and Without Pneumatic Chamber

The performance of rectangular shaped breakwaters with and without pneumatic chambers installed on them was studied by He *et al*. (2011). He *et al*. (2011) proposed a novel configuration of a pneumatic floating breakwater for combined wave protection and potential wave energy capturing. Pneumatic is a system that uses compressed air trapped in a chamber to produce mechanical motion for instance, a vacuum pump.

The development of the concept originates from the oscillating water column (OWC) device commonly used in wave energy utilization (Falcao, 2010). The configuration consists of the box-type breakwater with a rectangular cross section as the base structure, with pneumatic chambers (OWC units) installed on both front and back sides of the box-type breakwater without modifying the geometry of the original base structure as shown in Figure 2.5.

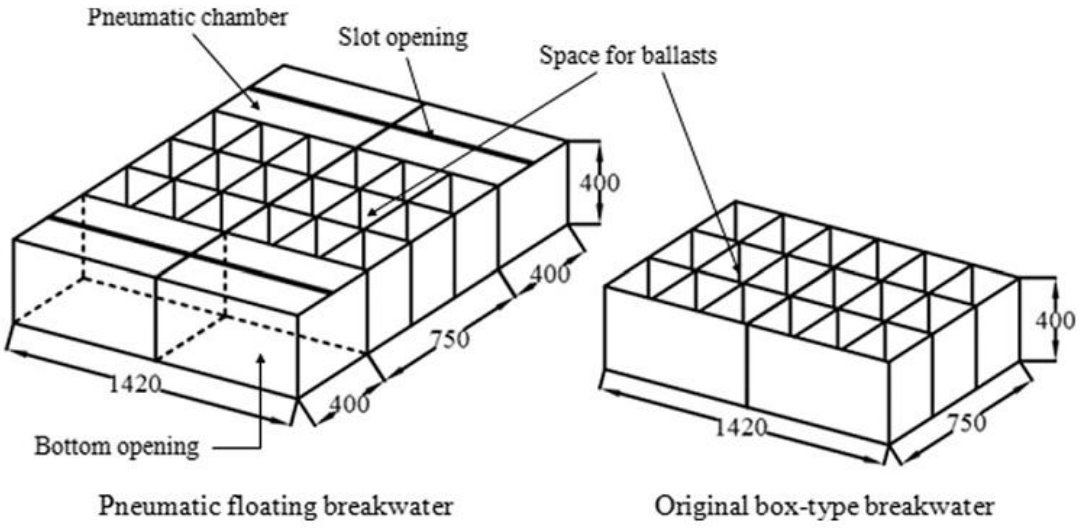

Figure 2.5: Pneumatic floating breakwater and box type rectangular (He *et al*., 2011)

The pneumatic chamber used in this experiment is of hollow chamber with large submerged bottom opening below the water level. Air trapped above the water surface inside the chamber is pressured due to water column oscillation inside the chamber and it can exit the chamber through a small opening at the top cover with energy dissipation. The aim for this experiment is to provide an economical way to

improve the performance of the box-type floating breakwater for long waves without significantly increasing its weight and construction cost. The performance was compared with that of the original box-type floating breakwater without pneumatic chambers. With the comparison of these two configurations, the wave transmission, wave energy dissipation, motion responses, the effect of draught and air pressure fluctuation inside the pneumatic chamber were studied.

From this study, with the installation of the pneumatic chambers, wave transmission coefficient was reduced in the whole range of *B/L*. This is because the pneumatic chambers changed the wave scattering and energy dissipation of incoming waves. Draughts were adjusted by extra ballast where model with deeper draught had a larger mass and larger moment of inertia and the amount of water in the pneumatic chamber were also increased. Deepening the draught reduced the wave transmission beneath the breakwater but increased the wave reflection.

2.6.3 Y-Frame Floating Breakwater

Mani (1991) studied different types of existing breakwaters performance in reducing transmission coefficient. It was determine that the "relative width" which is the ratio of width of the floating breakwater (*B)* to the wavelength (*L*) influence greatly the wave transmission characteristic of a breakwater. It was suggested that *B/L* ratio should be greater than 0.3 to obtain transmission coefficient below 0.5. Increment of width will cause the construction cost of the breakwater to increase and handling and installation of the breakwater will be more difficult.

Y-Frame floating breakwater was designed to reduce the width of the floating breakwater by changing its shape as shown in Figure 2.6 without incurring significant extra costs while improving the performance of the breakwater in reduction of the transmission coefficient. The inverse trapezoidal pontoon was selected with a row of pipe installed underneath. The aim for the installation of the row of pipes is to reduce *B/L* ratio and at the same time increasing the draft of the breakwater.

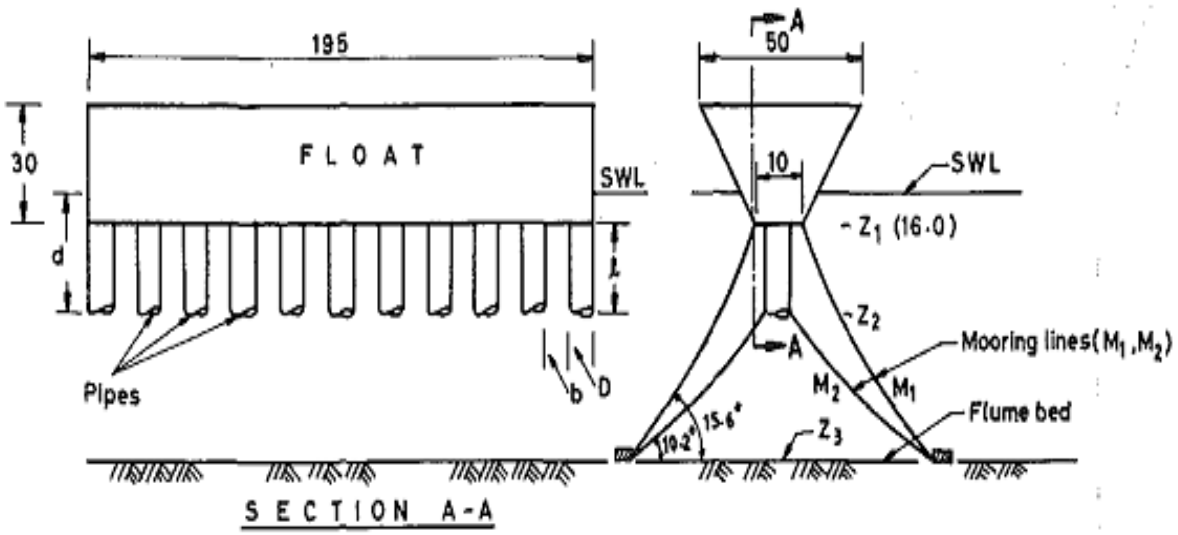

Figure 2.6: Details of the Y-Frame floating breakwater (Mani, 1991)

This study shows that closer spacing between pipes reduce transmission coefficient due to the improved reflection characteristic of breakwater and dissipation of wave energy due to turbulence created because of flow separation in the vicinity of the pipe. Thus attaching pipes at the bottom of the breakwater resulted in smaller *B/L* ratio, easy handling, minimum space occupied and acceptable value of transmission coefficient.

Mani (1991) also compared his results with similar experimental studies (Kato *et al.*, 1966; Carver & Davidson, 1983; Brebner & Ofuya; 1968; Bishop, 1982) as shown in Figure 2.7. From the comparison, it was deduced that the Y-frame floating breakwater performed well with row of pipes attached to the bottom of the trapezoidal float compared to other studies. The performance of the Y-frame floating breakwater attenuates waves better as transmission coefficient was decreased when the relative width ratio increased.

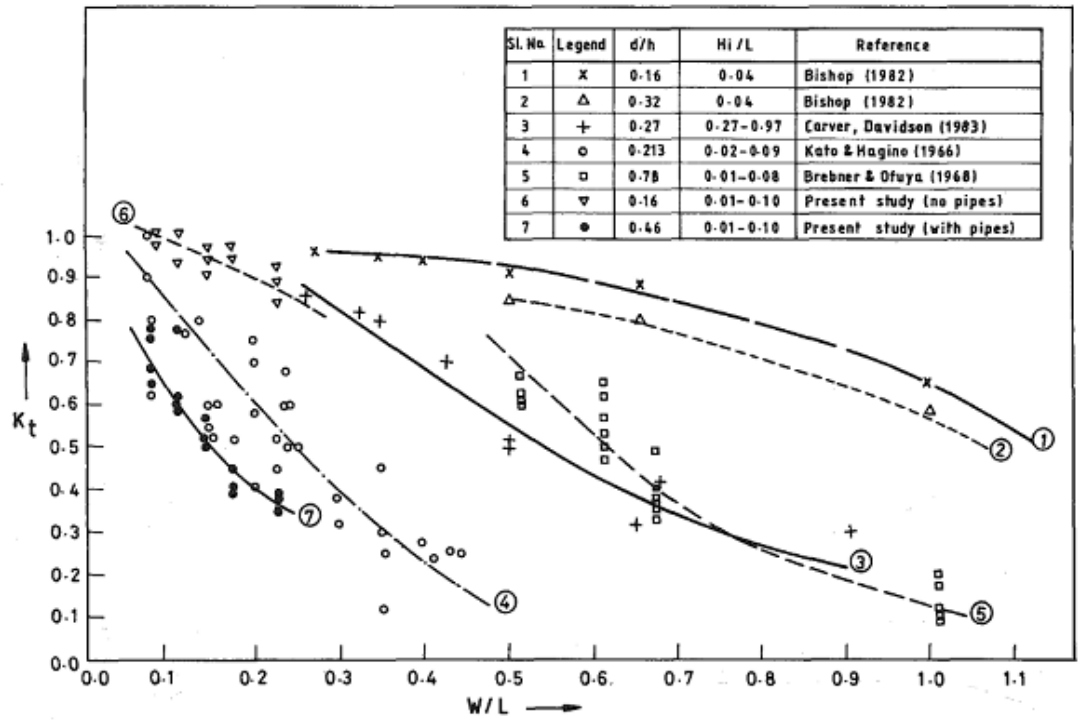

Figure 2.7: Comparison of variation of transmission coefficient with *B/L* (Mani, 1991)

2.6.4 Cage Floating Breakwater

Murali & Mani (1997) adopted the cost-effective Y-frame floating breakwater (Mani, 1991) in designing the cage floating breakwater which comprises two trapezoidal pontoons connected together with nylon mesh with two rows of closely spaced pipes as shown in Figure 2.8. The breakwater offers advantages such as easy on land fabrication, quick installation, less maintenance, and environmental friendly. The aim of this study is to investigate the effect of the new cage floating breakwater configuration on wave transmission coefficient.

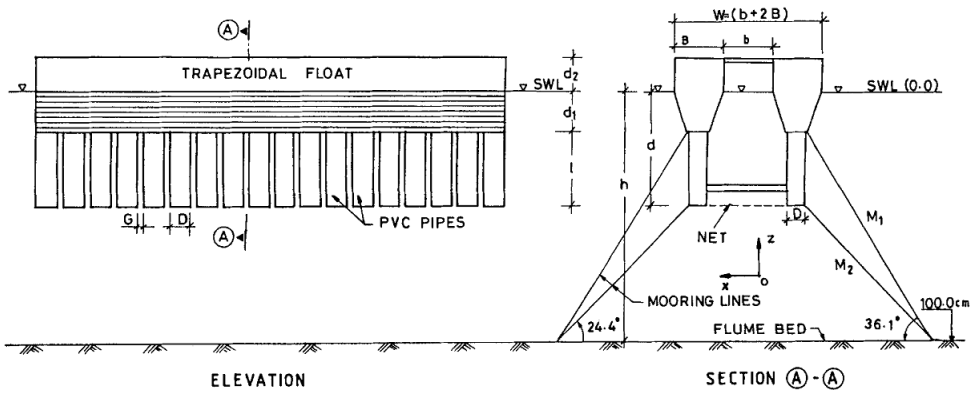

Figure 2.8: Cage floating breakwater (Murali & Mani, 1997)

Murali & Mani (1997) also compared their present design with previous studies (Kato *et al*., 1966; Brebner & Ofuya, 1968; Yamamoto, 1981; Bishop, 1982; Carver & Davidson, 1983; Mani, 1991) on the effects of *B/L* on C_t as shown in Figure 2.9. It shows that the curve 8 is the cage floating breakwater and it shows for C_t to be below 0.5, the recommended *B/L* ratio is 0.14 - 0.60. Comparison with the previous Y-frame breakwater design (Mani, 1991), curve 7 reveals that the cage floating breakwater is 10 - 20% more efficient in controlling the transmission coefficient.

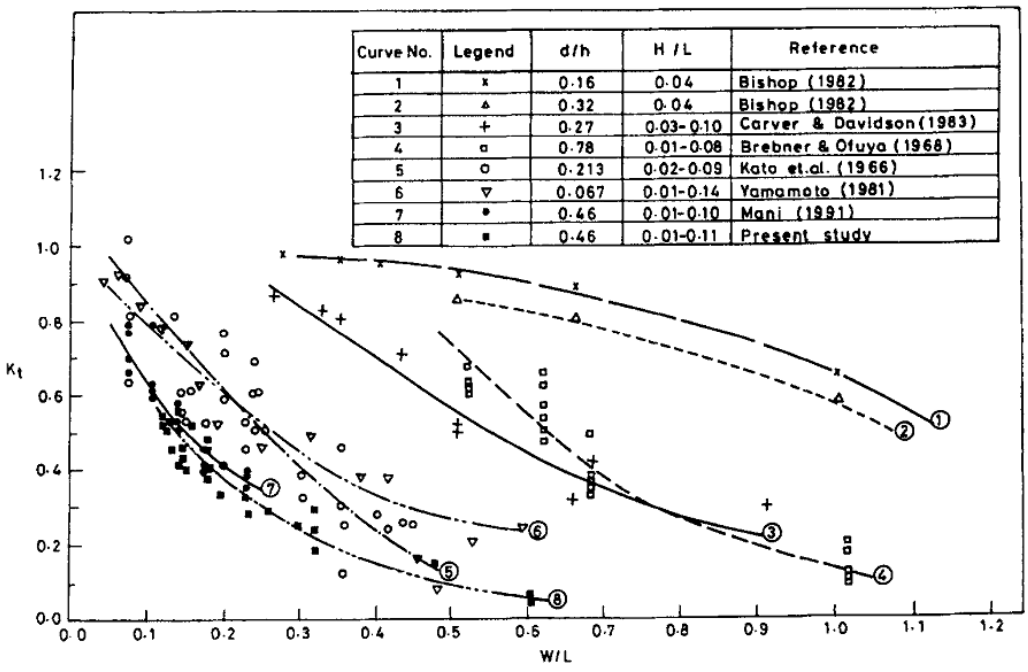

Figure 2.9: Comparison of the performance of floating breakwater (Murali & Mani, 1997)

2.6.5 Dual Pontoon Floating Breakwater (Catamaran)

Williams & Abul-Azm (1997) investigated the hydrodynamic properties of a dual pontoon breakwater consisting of a pair of floating cylinder of rectangular section connected by a rigid deck as shown in Figure 2.10. The effects of various waves and structural parameters on the efficiency of the breakwater as a wave barrier were studied. A boundary element technique was utilized to calculate the wave transmission and reflection characteristics.

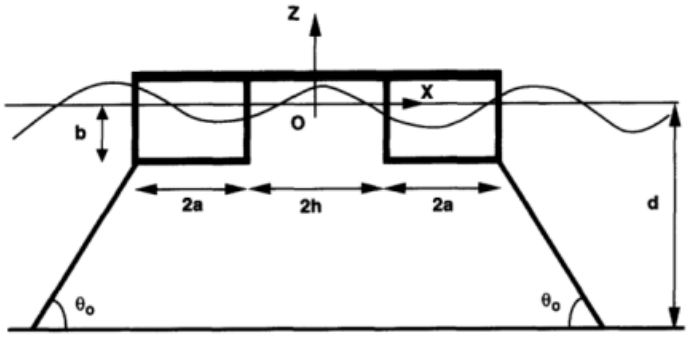

Figure 2.10: Dual pontoon breakwater sketch (Williams & Abul-Azm, 1997)

The performance of the dual pontoon structure depends upon the width (*2a*), draft (*b*), and spacing (*2h*) of the pontoons. Figure 2.11 shows the influence of pontoon draft on the reflection coefficient which shows that the larger the draft, the higher will be the reflection coefficient.

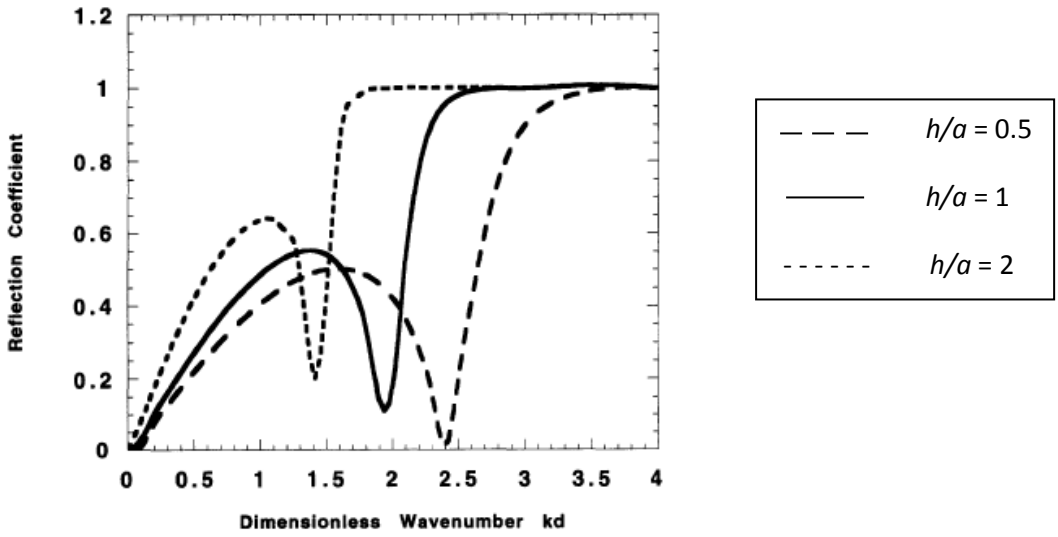

Figure 2.11: Influence of pontoon draft on reflection coefficient (Williams & Abul-Azm, 1997)

Figure 2.12 present the influence of pontoon width on the reflection coefficient which shows that as the width of pontoon increased, the reflection coefficient of the pontoon also increases.

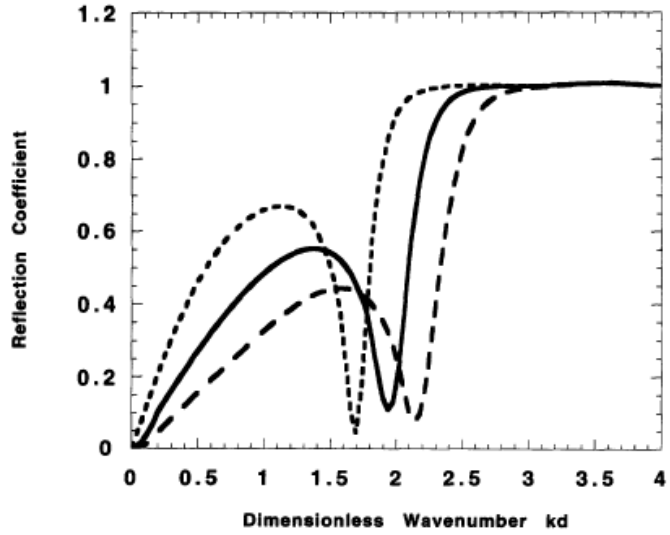

Figure 2.12: Influence of pontoon width on reflection coefficient (Williams & Abul-Azm, 1997)

Figure 2.13 show the effect of pontoons spacing on the reflection coefficient. The bigger the spacing between pontoon, the better will the breakwater perform because it acts as a continuous barrier in long waves and act independently in short waves.

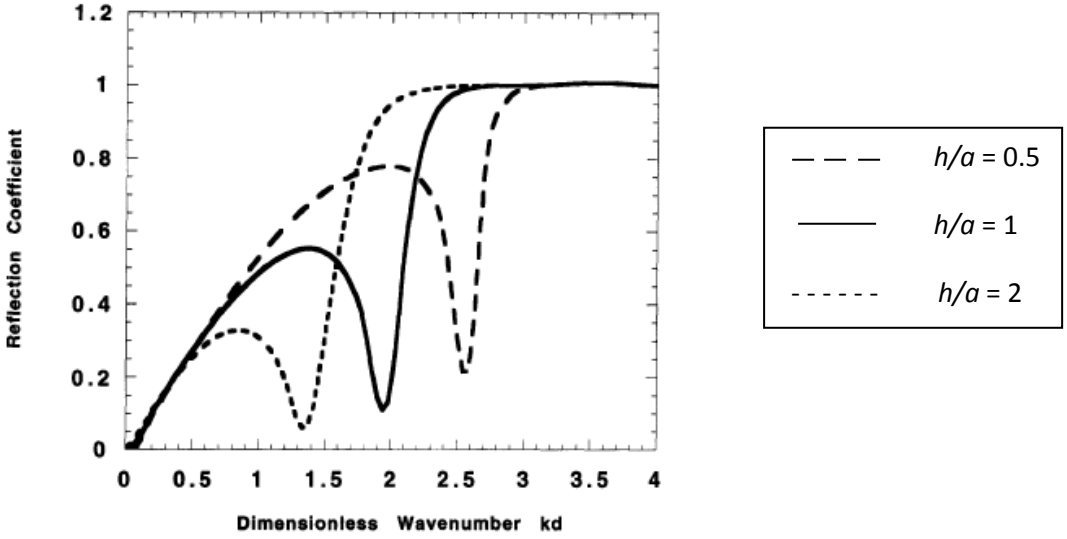

Figure 2.13: Influence of pontoon spacing on reflection coefficient (Williams & Abul-Azm, 1997)

When compared with the dual (lines) and single pontoon (Figure 2.14), Williams & Abul-Azm (1997) found that the dual pontoon exhibit high reflection coefficient in low frequency ($C_l < 0.75$ or $C_l < 1.0$) and mid frequency ($1.5 < C_l < 3.0$) range which shows that the dual pontoon is a more efficient wave barrier in lower and mid range frequency compared to the single pontoon. Williams & Abul-Azm (1997) found that wave reflection properties of the structure depend strongly on the draft and spacing of the pontoons.

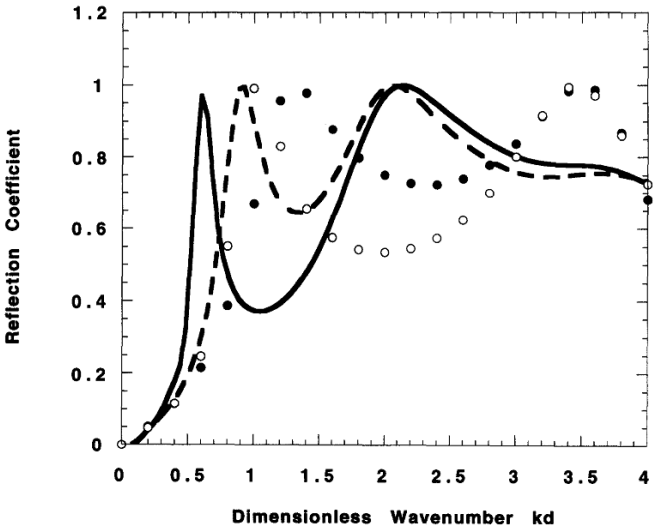

Figure 2.14: Comparison of reflection for dual pontoon structure (line) and single pontoon (symbol) of draft *b* and width (*4a+2h)* for *d/a* = 5, *b/a* = 1, *h/a* = 1, and *p* = 0.25. (Williams and Abul-Azm, 1997)

2.6.6 Dual Pontoon Floating Breakwater with Fish Net Attached

Tang *et al*. (2011) investigate the dynamic properties of a dual pontoon floating structure (DPFS) with and without a fish net attached as shown in Figure 2.14 by using physical and numerical models. In Figure 2.15, *a* is the pontoon width, *b* is the spacing between two pontoons, *d* is the draft, and *h* is the water depth. The purpose for attaching the fish net is to increase the draft of the structure and at the same time offering a room for marine aquaculture.

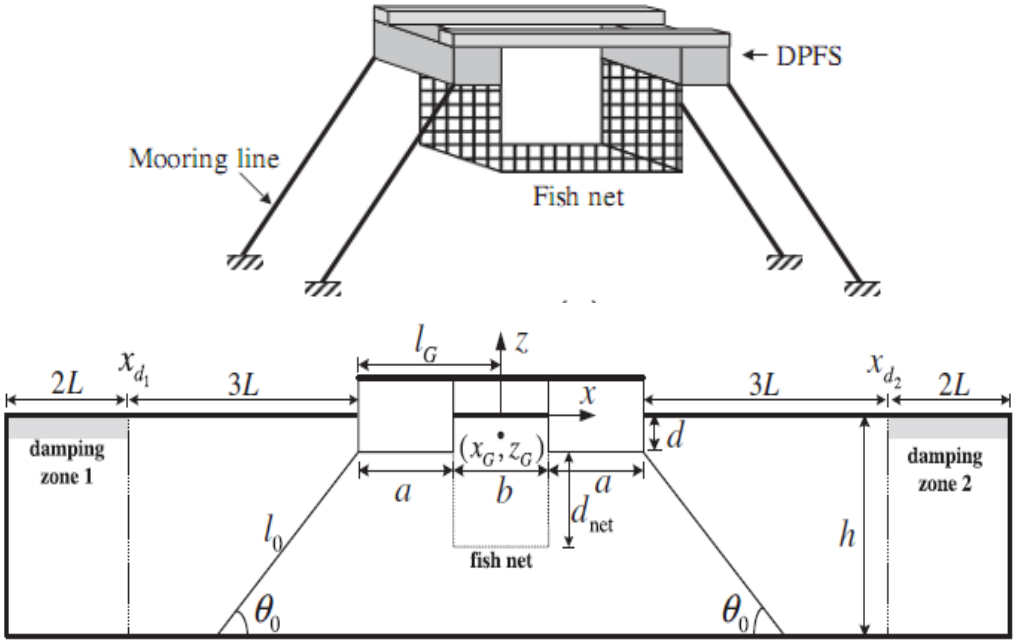

Figure 2.15: Dual pontoon floating breakwater with fish net attached (Tang *et al.*, 2011)

Figure 2.16 shows the comparison of the reflection coefficient with different net depths. The trend seems to be that the DPFS with deeper net has the lower reflection coefficient at the peaks due to the energy dissipated in the fluid-net interaction.

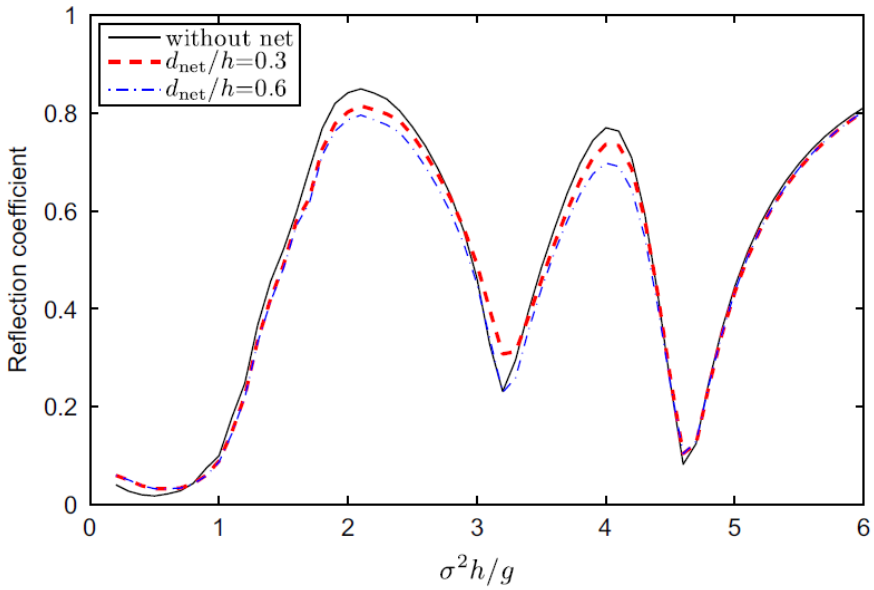

Figure 2.16: Comparison of reflection coefficient for the DPFS with different net depth. (Tang *et al*., 2011)

Figure 2.17 shows the comparison of the reflection coefficient of DPFS with different net width. Enlarging the width of the net would reduce the reflection coefficient because most of the wave energy was absorbed by the structure.

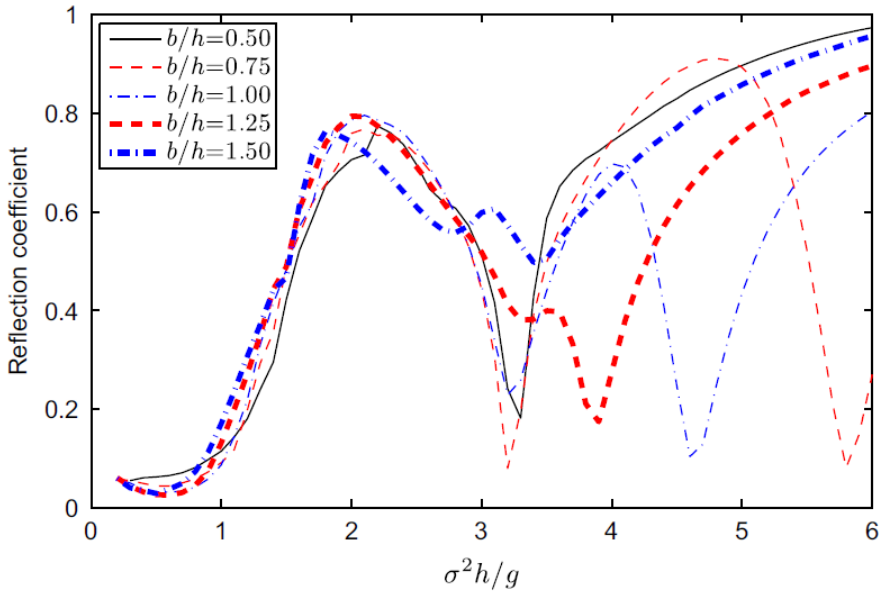

Figure 2.17: Comparison of reflection coefficient for the DPFS with different net widths. (Tang *et al.*, 2011)

2.6.7 Mat Type (Porous) Floating Breakwater

Mat type floating breakwater consists of a series of scrap tires or log rafts chained by a cable together and moored to the sea floor. Rubber tires floats well in water and the arrangement of the tires provide a semi-permeable surface which allows some wave energy to be reflected while the other half passed through the configuration and gets dissipated. Floating mat type breakwater offer disadvantages such as lack of buoyancy and unwanted marine growth and silt or debris accumulation in the tires that can sink the breakwater. The main reason for the implementation of this type of breakwater is due to low material and labor cost.

Wang and Sun (2010) developed a mat-type floating breakwater that consists of a large number of diamond-shaped blocks that was arranged to reduce transmitted wave height as shown in Figure 2.18. They also considered two different mooring

models which are directional mooring and bidirectional mooring as shown in Figure 2.19 and Figure 2.20 respectively.

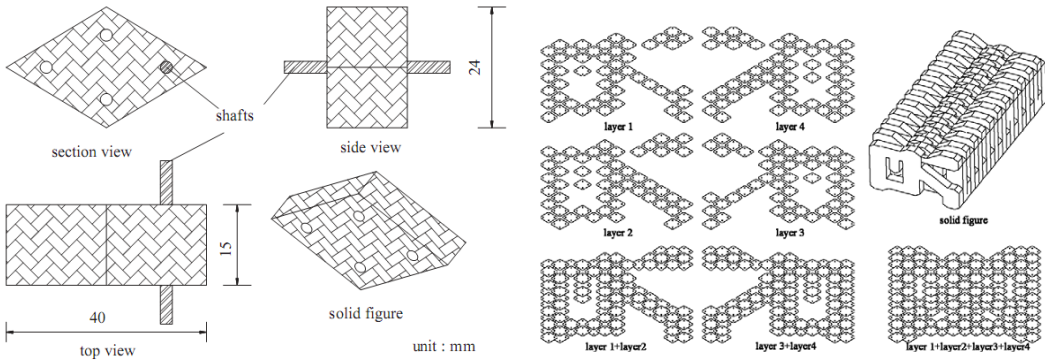

Figure 2.18: Sketch of diamond shape block (left) and arrangement of the blocks (right) (Wang & Sun, 2010)

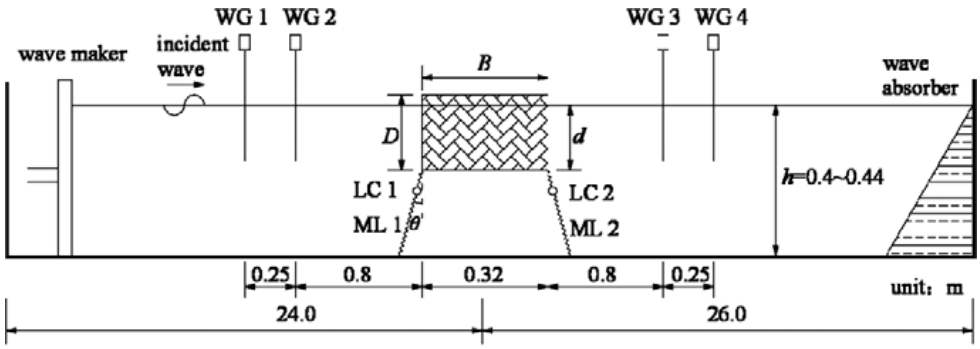

Figure 2.19: Experimental set-up with directional mooring. (Wang & Sun, 2010)

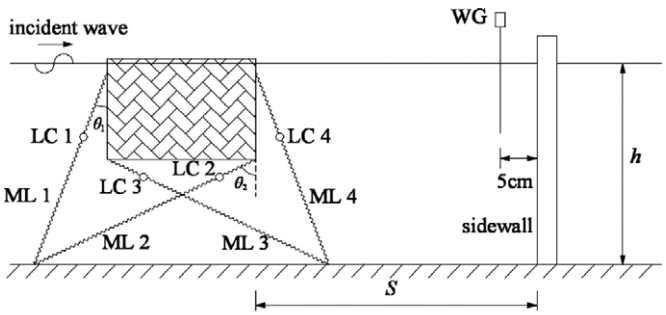

Figure 2.20: Bidirectional mooring (Wang & Sun, 2010)

For the directional mooring, the incident wave energy (E_{loss}) varies from 0.29 to 0.99 as *B/L* increases while in the bidirectional mooring, the (E_{loss}) varies from 0.69 to 0.99 which shows that the bidirectional mooring which fraps the floating body tighter than the directional mooring, brings not only preferable E_{loss} but also enhanced mooring force. The transmission coefficient of the floating breakwater decreased and the dissipation of wave energy increases with the increase of *B/L* (C_t is less than 0.5 and E_{loss} is higher than 0.78 as *B/L* is higher than 0.323).

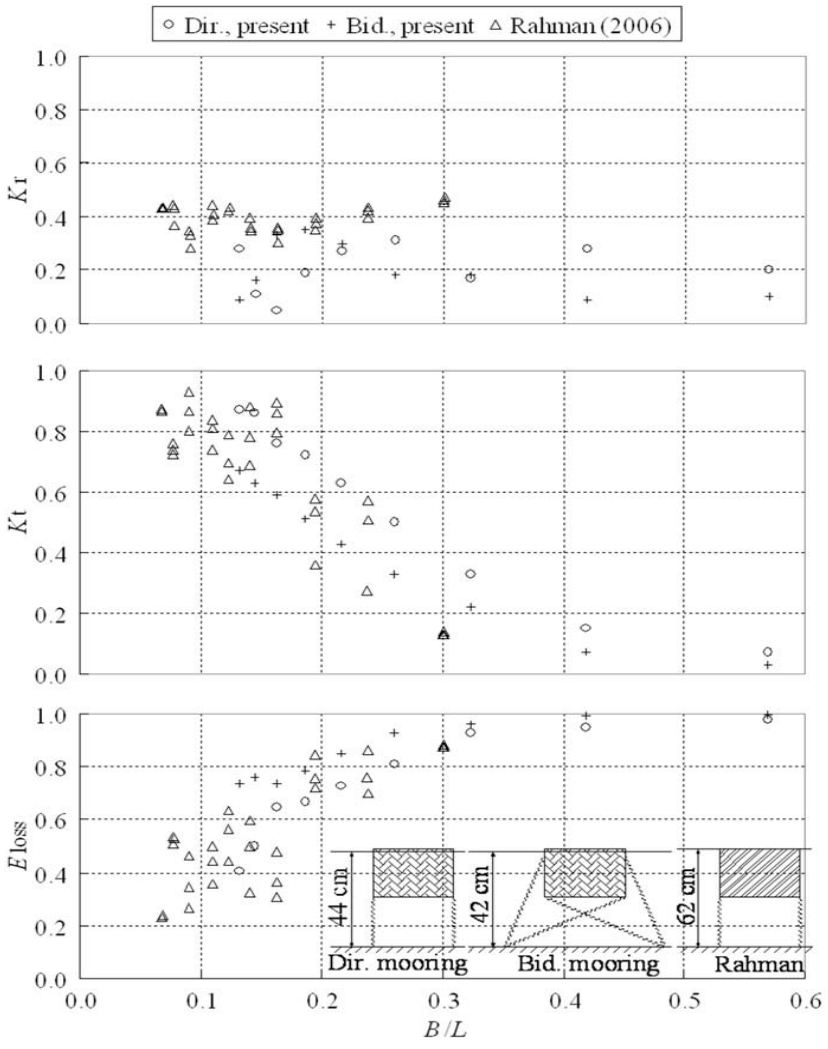

Figure 2.21: Comparison between Wang and Sun result, and that of the conventional pontoon breakwater (Rahman *et al.*, 2006) on reflection coefficient (C_r), transmission coefficient (C_t) and wave energy dissipation (E_{loss}). (Wang and Sun, 2010)

As shown in the Figure 2.21 above, Wang and Sun (2010) also did a comparison with the conventional pontoon floating breakwater (Rahman *et al*., 2006) on transmission, reflection and energy dissipation. It was shown that for the directional mooring, the reflection coefficient and transmission coefficient of porous floating breakwater are lower and higher than that of conventional pontoon breakwater. However there is no significant E_{loss} between them. The porous floating breakwater with bidirectional mooring present lower C_r , higher E_{loss} and lower C_t when compared with the pontoon breakwater (Rahman *et al*., 2006).

2.6.8 Tethered Float Breakwater

Vethamony (1995) studied the wave attenuation characteristics of a tethered float system as shown in Figure 2.22, with respect to wave heights, wave periods, wave depths, depths of submergence of float and float size. From this experiment, it was determined that the efficiency of the tethered float system was at maximum when it was just submerged but decreased when depth of submergence (d_s) of float increases. The wave attenuation denoted by transmission coefficient (C_t) decreased with the increase in float size (r). For any level of wave attenuation, float array size decreases with decrease in float size. The smaller the float size, the higher will be the wave attenuation, since small floats undergo maximum excursion and interfere with the orbital motion of the fluid particles.

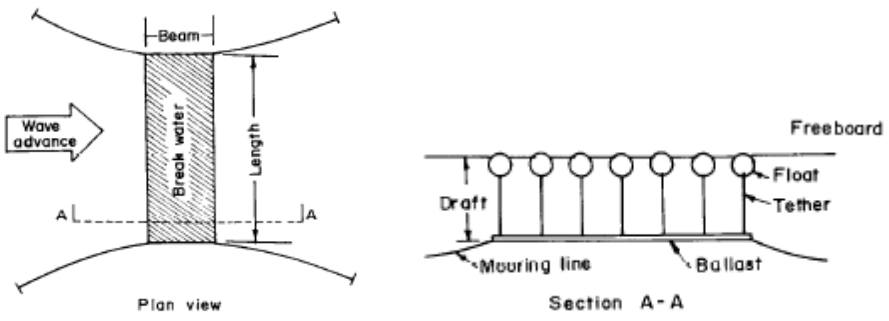

Figure 2.22: Tethered float breakwater (Vethamony, 1995)

2.6.9 H-Type Floating Breakwater (H-Float)

Teh & Nuzul (2013) studied the hydraulic performance of a newly developed H-type floating breakwater (Figure 2.23) in regular waves. The aim of this study was to conduct a laboratory test to determine the wave transmission, reflection and energy dissipation characteristics of the breakwater model under various wave conditions. The breakwater was previously developed by a group of UTP students for their Engineering Team Project in 2004. The breakwater was designed to reduce wave energy through reflection, wave breaking, friction and turbulence. The two "arms" at the top of the main body was create to facilitate wave breaking at the structure; whereas the two "legs" at the bottom was created to enhance the weight of the breakwater barrier against wave actions.

The breakwater model was made of autoclaved lightweight concrete (ALC) with fiberglass coating. According to Teh & Nuzul (2013), wave transmission coefficient, C_t decrease with the increasing *B/L* ratio. The H-type breakwater was capable of dampening the incident wave height by almost 80% when the breakwater was designed at *B/L*= 0.5. The H-type breakwater was less effective in dampening longer waves in the flume. The H-type breakwater was capable in attenuating *90%* of the incident wave height when *B/L* is approaching *0.4*. However, the experiment were conducted in limited wave range due to time constrains.

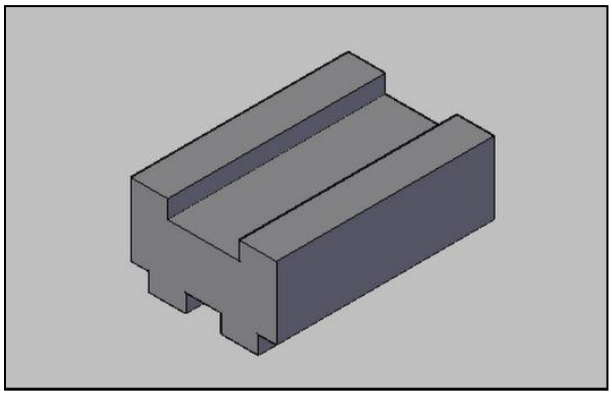

Figure 2.23: H-type floating breakwater (H-float)

2.7 PERFORMANCE OF OTHER EXISTING FLOATING BREAKWATER

2.7.1 Experiments on Wave Transmission Coefficients of Floating Breakwaters

Dong *et al.* (2008) studied the wave transmission coefficients of the three types of breakwaters which is single box, double box and the board net. These three floating structures are studied under regular waves with or without currents. As shown in Figure 2.24, the single box floating breakwater is a simple box with dimension of 20 m width x 4.8 m height. While the double box floating breakwater includes two identical single boxes connected by rigid thin boards. The board net floating breakwater is a thin plane board with several rows of net underneath.

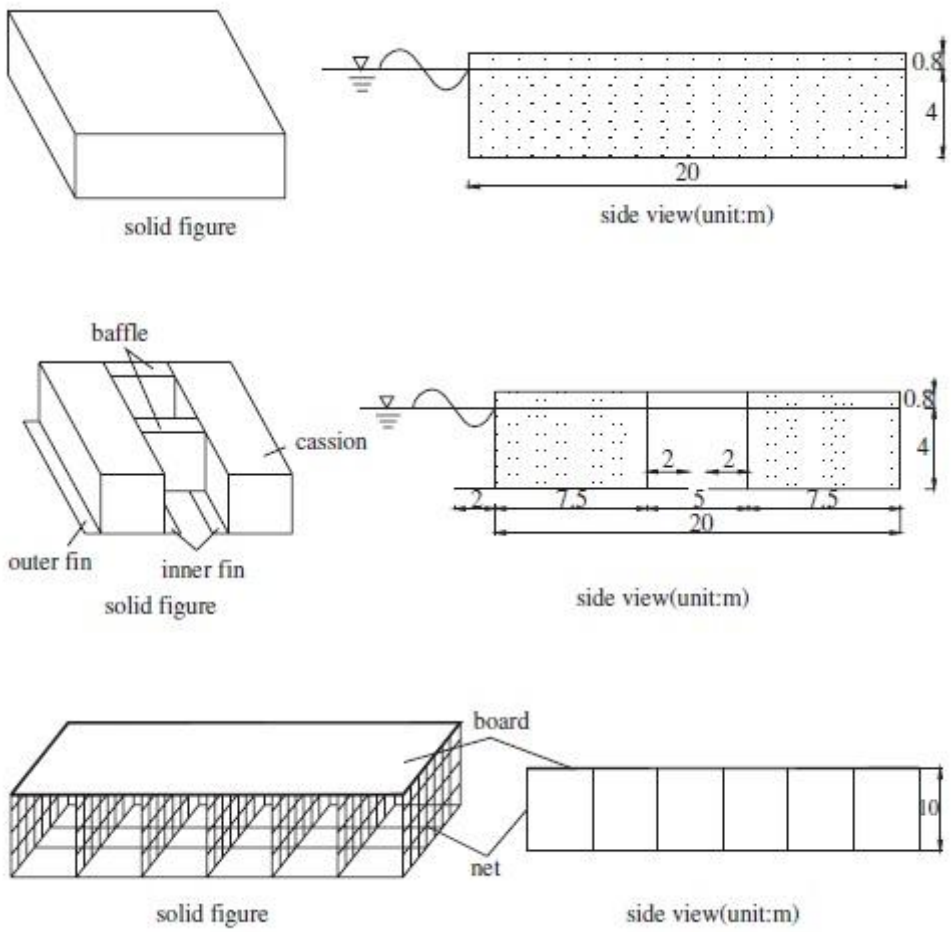

Figure 2.24: The single box FBW; The double box FBW; The board net FBW (Dong *et al.*, 2008)

In this experiment, the single box breakwater is connected to the sea bed by mooring chains and was adjusted to determine the length of the chain lying (LCL). The LCL did apparently affect the transmission coefficient because the structure was more restricted by the mooring chains with 10 m of LCL and thus blocked more wave energy.

For the double box breakwater, it is proved by Dong *et al.* (2008) that it can reduce the wave height more than the single box. However, if small wave transmission coefficient is needed, then the width of the breakwater must be greatly widened, which in turn would require more materials and stronger mooring system.

There is no doubt that nets have effectively reduced the wave height. So, an improvement has been made to the board to increase its rigidity by fixing several slender reinforcing steel bars underneath it. Based on the test results, it shows that the wave transmission coefficients were reduced by increasing the rigidity of the board, especially for long waves.

2.7.2 Experimental Study on the Performance Characteristics of Porous Perpendicular Pipe Breakwaters

Shih (2012) investigated the dissipation and wave transmission of porous perpendicular pipe breakwaters with different wave conditions and various diameter and tube length. This porous breakwater is tested by using regular waves to assess the efficiency and proves the design concept. As shown in Figure 2.25, the pipe breakwaters were placed parallel to each other without spacing in between and longitudinally parallel to the direction of incident waves.

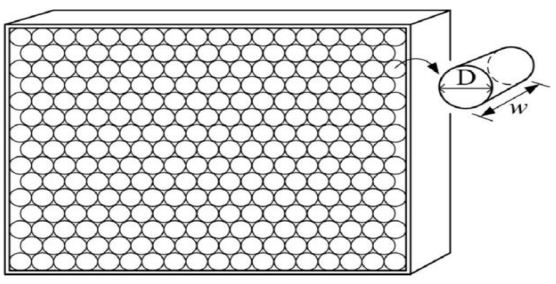

Figure 2.25: Sketch diagram of pipe breakwaters (Shih, 2012)

Based on the results obtained, it can be said that a longer pipe for this structure can reflect more incident waves, which mean it can reduce the reflection coefficient better. Besides, shorter pipe lengths will attenuate shorter incident waves well, but perform poorly for longer wave. The results of the experiment also implied that reflection of the pipe breakwater is slightly affected by the pipe diameter, but minor diameter can create higher substantive attenuation.

CHAPTER 3

METHODOLOGY

This chapter deliberates the development of H-type floating breakwater (H-Float) and its physical properties. The equipment and instrument that are used to test the model are also presented. The materials used for the H-Float model construction as well as the experimental set-up will be thoroughly discussed. Besides, this chapter also will deliver the project activities and Gantt chart for the overall study of H-Float.

3.1 MODEL DESCRIPTION OF THE H-TYPE FLOATING BREAKWATER

In this study, H-Float is developed with a scale of 1:15. The design of this H-Float is the continuation of the past study done by other UTP students. The new design for the H-float will include some enhancement and improvement based on the previous study, as well as the introduction of new configuration of mooring system.

The general dimension of the H-Float is 500 mm width x 1440 mm length x 250 mm height (Figure 3.1). The model was constructed by using plywood material and coated with fiberglass. Plywood is used because it is a naturally lightweight material that will keep the model afloat while the fiberglass coating will act as water-proof membrane to prevent water from seeping into the model. The fiberglass coating is mixed with yellow coloring pigment for better visibility of the model during the experiments.

As shown in Figure 3.2, the H-Float has a pair of upward arms and a pair of downwards legs, both are attached to the breakwater body. The upward arms act as the frontal barrier in withstanding the incident wave energy mainly by reflection. Some wave energy is anticipated to be dissipated through vortices and turbulence at the 90^{o} frontal edges of the breakwater. When confronted by storm waves, the H-Float permits water waves to overtop the seaward arm and reaches the U-shape body. The

overtopped water trapped within the U-shape body heavily interacts with the breakwater body, and the flow momentum is subsequently retarded by shearing stresses (frictional loss) developed along the body surfaces. The excessive waves in the U-shape body may leap over the shoreward arm and reaches the lee side of the floating body, making a new wave behind the breakwater which is termed as the transmitted waves.

The downward legs of the H-Float act as the secondary barrier against incoming waves by obstructing the wave motion beneath the breakwater. Both legs (seeward and leeward), which are constantly immersed in water, are particularly useful in intercepting the transmission of wave energy beneath the floating body.

On the other hand, as breakwater immersion depth is an important parameter in controlling the hydrodynamic performance of the H-Float, a ballast chamber located within the breakwater body was designed for adjustment of immersion depth of the breakwater with respect to still water level, in a freely floating condition. Matrix wooden grid system was developed for the placement of sandbags in order to control the weight of the breakwater. The ballast chamber was covered by transparent lid made of Plexiglas. The gap between the breakwater body and the transparent lid was tightly sealed by adhesive tapes so as to prevent the seepage of water to the ballast chamber.

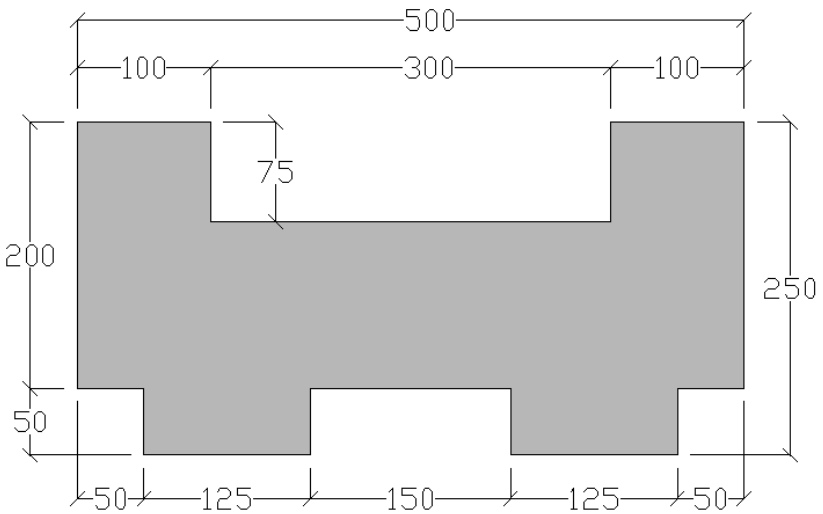

Side View of Outer Body

Figure 3.1: Side view of H-float outer body

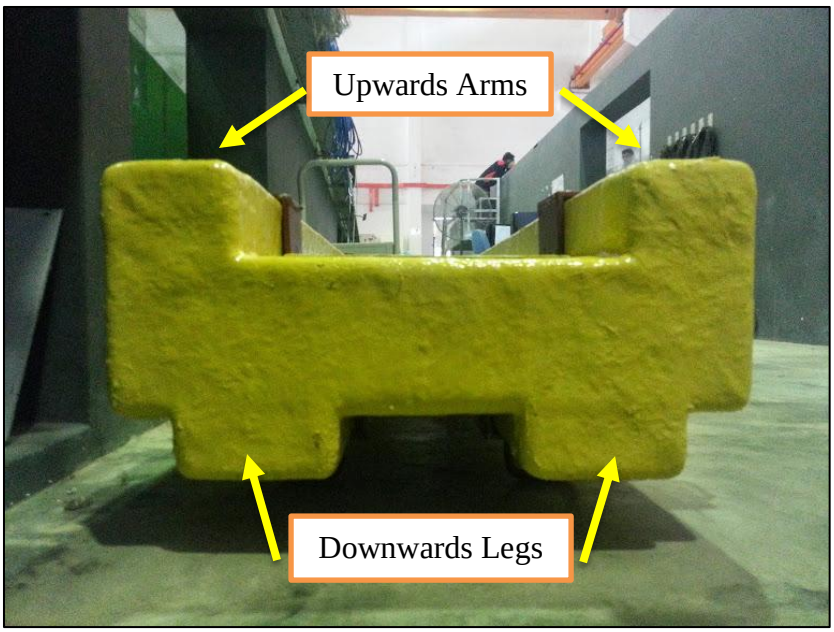

Figure 3.2: Cross section of the breakwater outline

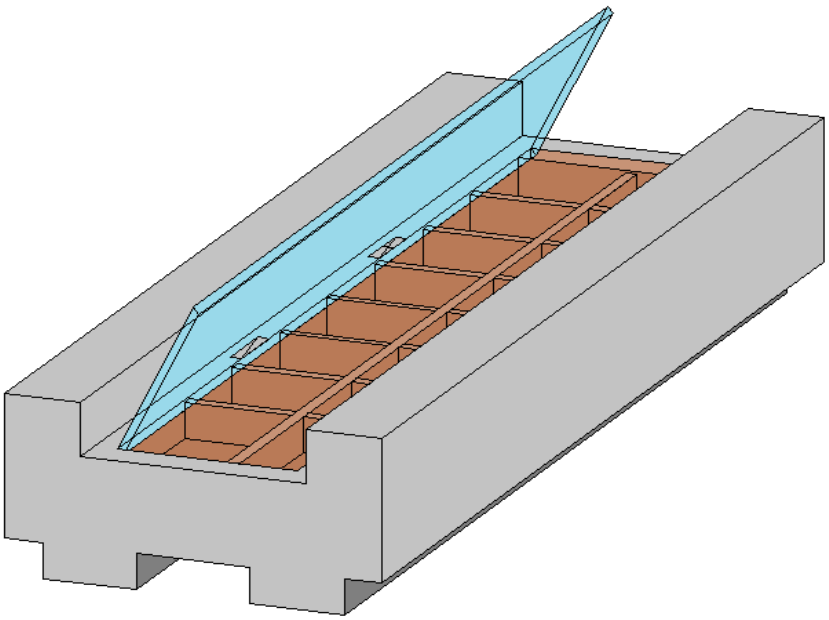

Figure 3.3: Isometric view of the model

Figure 3.4: Fabricated H-float model

The sides of the breakwater facing the tank walls are covered with polystyrene foam board to prevent direct collision between the concrete wall and the H-Float body, which can damage the body structure. The implementation of the polystyrene foams at both sides of the breakwater would not pose significant disturbance to the movement of the floating body.

3.2 MOORING SYSTEM CONFIGURATION

In this study, mooring system is considered as one of the important aspect to ensure that the H-Float can be held in the desire position. There are two types of mooring system used, which are taut leg system and catenary system. Taut leg system is used in this test since it gives the test model up to six degree of freedom movement, for the hydrodynamic performance. In this system, a thin metal rope or cable with low elasticity is used as the mooring line, connected from the H-Float body to the anchor located at the floor of the wave tank. Such configuration will give the mooring line a pre-tensile stress prior to the test conducted. The H-Float is moored with bidirectional mooring for this mooring system. There are total of four hooking point on each side of

the breakwater body. This time, the model is installed with a pair of hook frame, as shown in Figure 3.5.

Figure 3.5: Hook frame installed to the breakwater body

Meanwhile, the second part of the experiment used the catenary mooring system as it provides restoring forces through the suspended weight of the mooring lines and its change in configuration arising from vessel motion. Directional mooring is applied in this system. Figure 4.1 and 4.2 in Section 4.2 shows the differences between taut leg system and catenary system.

3.3 TEST EQUIPMENT

The study of H-Float is conducted in Offshore Laboratory (Block A) at Universiti Teknologi PETRONAS (UTP). The main facilities that is used and provided in the Offshore Laboratory of UTP is the wave tank, with the latter part being the key facility for this study. Other equipment that are used in this study such as wave probes, wave absorber and wave generator are provided in the laboratory as well.

3.3.1 Wave tank

The tests for H-Float are conducted in the modified wave tank with a dimension of 25 m long, 1.5 m wide and 3.2 m high as shown in Figure 3.6. The maximum water level that can be fill in the flume is up to 1.2 m high. The wave tank is made of reinforced concrete for its wall and 6 strong Plexiglas panel at both side of the flume. The presence of these glasses will make it easier to observe the wave interaction with the model tested. Partitions are arranged in the wave tank according to the dimension that is specified.

Figure 3.6: Wave tank

3.3.2 Wave Generator

Wave generators are equipped at the one end of the wave tank and are used to generate both regular and random waves, as shown in Figure 3.7. It has the capability of generating waves up to 2 second wave period, and maximum wave heights of 0.3

m. The wave generator was manufactured by the HR Wallingford. The control of the wave generator is operated using ocean and wave software supplied by HR Wallingford. To generate waves in the wave tank, command signals coded using the program needs to be properly compiled to facilitate the computation of a wave elevation time series corresponding to the desired state that need to be carried out upon the tests. For this test, three wave generators are used to generate the regular and random waves.

Figure 3.7: Wave generator

3.3.3 Wave Absorber

Wave absorber is placed at the other end of the wave tank with the purpose of absorbing the remaining wave energy from the waves generated by the wave paddle and also minimizing the reflected waves in the wave tank. This device is important to avoid any errors to the readings of reflected and transmitted wave heights due to remaining wave energy of the previous waves. Figure 3.8 shows the wave absorber which is made of anti-corrosion material with the ability to absorb up to 90% of wave energy.

Figure 3.8: Wave absorber

3.3.4 Wave Probe

As shown in Figure 3.9, wave probes are used to measure the incident wave height, reflected wave height and transmitted wave height at the seaward and leeward side of the model. Three wave probes are installed in front of the model which faces the incident waves to measure the incident and reflected wave data while at the leeward side of the breakwater, another three wave probes are placed to measure the transmitted wave height. The maximum measurement of wave height is 0.4 m and 128 Hz for wave frequency. Calibration of probes is done prior to conduct any tests to avoid measurement errors.

Figure 3.9: Wave probes

3.4 EXPERIMENTAL SET-UP

Based on Figure 3.10, it shows the experimental set-up and the location of each equipment used to run the test. The H-Float model is located at the mid-length of the wave tank. The model is anchored to the floor of the wave tank with metal cables and hooks. Three wave probes are located on each side of the H-Float (seaward and leeward) to measure the water the water level fluctuation. The data collected by the wave probes will be analyzed to yield some significant wave parameters such as wave height, peak wave period and etc. All the six wave probes are arrange according to the Mansard and Funke's method (1985).

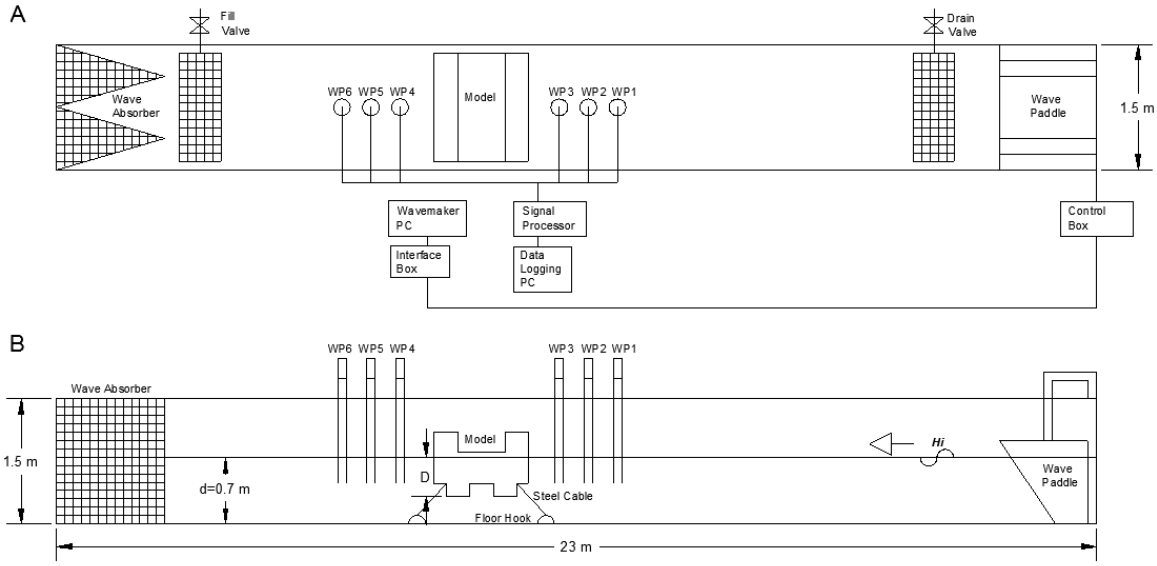

Figure 3.10: Plan and side view of the experiment set-up

3.5 EXPERIMENTAL CONFIGURATION

In this study, the H-Float model are tested against three manipulated variables which are wave periods, wave heights and mooring system. The testing of the model are done for both regular and random waves. In each of the variables, the values of each parameters are varied. For each mooring system, the model are tested at different

wave period. In each wave period, the H-Float model are tested at different wave height. The total number of test for regular and random waves are 84 tests for both taut leg and catenary mooring system. The variables that are used in this test are listed in the Table 3.1.

Table 3.1: Parameters/variables used in the testing

			Wave Steepness, H/L		**0.04**	**0.05**	**0.06**
Type of Mooring System	**Type of Wave**	**Water Depth (m)**	**Wave period, T (s)**	**Frequency, f**	**Wave Height (m)**	**Wave Height (m)**	**Wave Height (m)**
Taut Leg & Catenary	**Regular**	0.73	0.8	1.25	0.04	0.05	0.06
			0.9	1.11	0.05	0.06	0.08
			1.0	1.00	0.06	0.08	0.09
			1.1	0.91	0.08	0.09	0.11
			1.2	0.83	0.09	0.11	0.13
			1.3	0.77	0.10	0.13	0.15
			1.4	0.71	0.11	0.14	0.17
			1.5	0.67	0.13	0.16	0.19
			1.6	0.63	0.14	0.17	0.21
			1.7	0.59	0.15	0.19	0.23
			1.8	0.56	0.16	0.20	0.25
Taut Leg & Catenary	**Random**	0.73	0.8	1.25	0.04	0.05	0.06
			1.0	1.0	0.06	0.08	0.09
			1.2	0.83	0.09	0.11	0.13

3.6 TEST EQUIPMENT CALIBRATION

The calibration of the wave flume is done to check on the working condition of the flume as a whole, including the water pumping ability and the operation of equipment and devices required to complete this study.

Besides, wave probes also are calibrated in accordance to Mansard and Funke's (1985) 3-point method as mention earlier in the previous subtopic. The basic

of this method is to simultaneously measure the waves generated in the flume at three different points, each at both sides of the model, with adequate distance between one set of probe to another. The wave probes are located parallel to the wave's direction and perpendicular to the wave paddle in the wave flume.

The set-up of the wave probes calibration is shown in Figure 3.11 below. The distance from the wave paddle to Probe 1 is denoted by X1. The length of Probe 1 to the Probe 2 is denoted as X12 while the distance between Probe 1 and Probe 3 is denoted as X13.

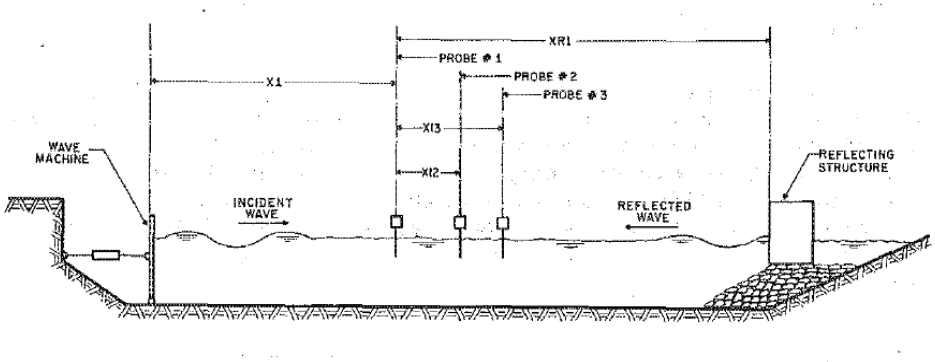

Figure 3.11: Three-point calibration set-up (Mansard and Funke, 1985)

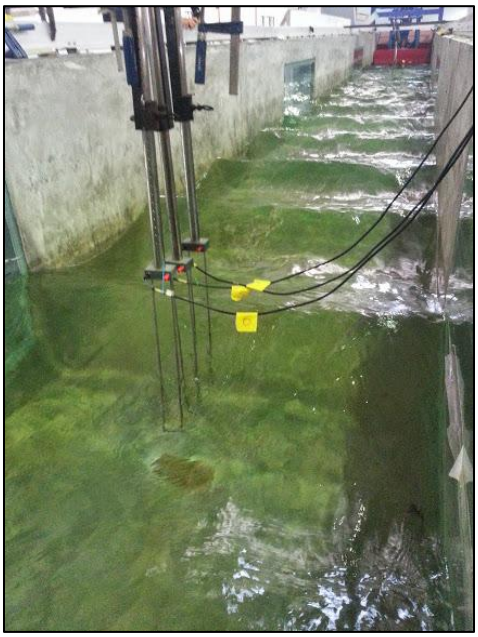

Figure 3.12: Calibration of wave probes

Table 3.2: Wave probes separations using Mansard and Funke's method (1980)

T (s)	f (Hz)	X_{12} (mm)	X_{23} (mm)	X_{13} (mm)
0.8	1.25	100	130	230
0.9	1.11	126	280	406
1.0	1.00	155	280	435
1.1	0.91	186	280	466
1.2	0.83	200	280	480
1.3	0.77	217	280	497
1.4	0.71	249	400	649
1.5	0.67	281	400	681
1.6	0.63	312	400	712
1.7	0.59	343	400	743
1.8	0.56	373	500	973

3.7 PROJECT KEY MILESTONES

In order to complete the Final Year Project titled "Effects of Mooring Configuration on Hydraulic Performance of the H-Type Floating Breakwater (H-Float) in Regular and Random Waves", few prominent activities will be carried out to ensure the feasibility of the study. These set of tasks are done in a number of stages to ensure the unobstructed flow of project.

i) Literature review

ii) Design of floating breakwater

iii) Fabrication of models

iv) Experiment set-up

v) Laboratory tests

vi) Result interpretation

vii) Validation of results

viii) Conclusion

3.8 PROJECT TIMELINE (GANTT CHART)

In the first half of the study, the focus is more on the introduction and preparation towards the further study of the test model. Besides, observation on experiment also being done for the existing model conducted by the previous student. This help to understand how the experiment is being conducted. As shown in Table 3.2, Gantt chart will help this study to keep on track of the progress work.

Table 3.3: Gantt chart

	Months	January				February				March				April				May				June				July				August				September			
	Weeks	1	2	3	4	5	6	7	8	9	10	11	12	13	14	15	16	17	18	19	20	21	22	23	24	25	26	27	28	29	30	31	32	33	34	35	36
1	Selection of project topic																																				
2	Preliminary research work																																				
3	Submission of extended proposal																																				
4	Proposal defense																																				
5	Design and fabrication of floating breakwater																																				
6	Submission of interim report																																				
7	Calibration equipments and experiments																																				
8	Submission of progress report																																				
9	Continuation of project report																																				
10	Pre-SEDEX																																				
11	Submission of draft final report																																				
12	Submission of dissertation (soft copy)																																				
13	Submission of technical paper																																				
14	Oral presentation (Viva)																																				
15	Submission of dissertation (hard bound)																																				

CHAPTER 4

RESULTS AND DISCUSSIONS

In this chapter, a brief explanation on the calibration of experimental study which is the gain value of the wave generator is delivered. Then, the effects of the type of mooring systems used is studied followed by the experimental results on the performance of H-Float and its analyses. These analyses are important in providing better understanding and also interpretations of the results gained after the experiments are completed. The details of the analyses are to be thoroughly discussed later in this chapter followed by short conclusion at the end.

4.1 GAIN VALUE

After setting up some of the test equipment, the experimental calibration need to be done in order to set the program of the software according to the variables calculated. The study of H-Float is carried out against random wave and also regular wave. Random wave is used to simulate realistic sea condition while regular wave is used to simulate a controlled environment of the sea. To program specific wave height in the wave generation software for each wave period, first run with gain 1.0 is carried out in the wave tank for 20 seconds (regular wave) or a few minutes (random wave). Then after that, the height of waves generated by the paddles are calculated and compared with the required wave height. If the height is not the same, then the run need to be carried out again with the new gain value. To calculate the gain value, simply divide the theoretical wave height with the experimental wave height.

For example:

Theoretical wave height = 0.15m

Experimental wave height = 0.13m

Gain value = 0.15m/0.13m = 1.15

This gain value is considered as an important tool in generating specific wave height accurately and must be done prior to varying periods and experimental settings. Table 4.1 and 4.2 shows the corresponding gain value for each wave height with various wave periods for random and regular waves.

Table 4.1: Gain value for corresponding wave height and periods (random wave)

Wave Steepness, H/L		0.04		0.05		0.06	
Wave period, T (s)	Frequency, f	Wave Height (m)	Gain Value	Wave Height (m)	Gain Value	Wave Height (m)	Gain Value
0.8	1.25	0.04	1.22	0.05	1.21	0.06	1.21
1.0	1.0	0.06	1.30	0.08	1.30	0.09	1.30
1.2	0.83	0.09	1.30	0.11	1.30	0.13	1.40

Table 4.2: Gain value for corresponding wave height and periods (regular wave)

Wave Steepness, H/L		0.04		0.05		0.06	
Wave period, T (s)	Frequency, f	Wave Height (m)	Gain Value	Wave Height (m)	Gain Value	Wave Height (m)	Gain Value
0.8	1.25	0.04	0.84	0.05	0.85	0.06	0.86
0.9	1.11	0.05	0.86	0.06	0.87	0.08	0.84
1.0	1.00	0.06	0.77	0.08	0.77	0.09	0.81
1.1	0.91	0.08	0.75	0.09	1.10	0.11	1.07
1.2	0.83	0.09	0.96	0.11	1.00	0.13	0.97
1.3	0.77	0.10	1.00	0.13	0.90	0.15	0.90
1.4	0.71	0.11	0.87	0.14	0.86	0.17	0.89
1.5	0.67	0.13	1.03	0.16	1.02	0.19	1.03
1.6	0.63	0.14	0.96	0.17	0.95	0.21	0.87
1.7	0.59	0.15	0.86	0.19	0.86	0.23	0.89
1.8	0.56	0.16	0.97	0.20	1.00	0.25	1.0

4.2 TYPE OF MOORING SYSTEM

The effects of mooring system is studied by experimenting the H-Float with two types of mooring system which are taut leg and catenary. Taut leg system is a mooring line that is pre-tensioned until it is taut. By this system, the mooring line terminates at an angle at the ground. Meanwhile, catenary system refers to the line

that is hanging free, assuming it is under the influence of gravity. The catenary system provides restoring forces through the suspended weight of the mooring lines and its change in configuration arising from vessel motion. The taut leg system used in this experiment is moored with bidirectional mooring while catenary system used is moored with directional mooring. Figure 4.1 and 4.2 shows the difference between taut leg system and catenary system.

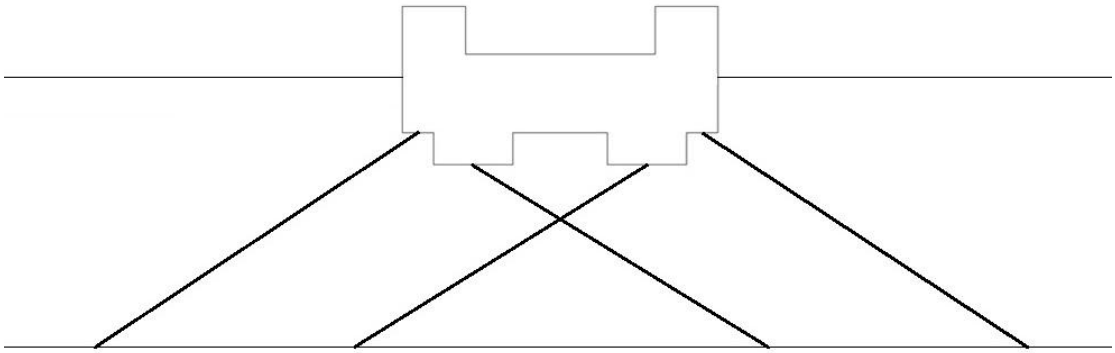

Figure 4.1: Taut leg system (bidirectional mooring)

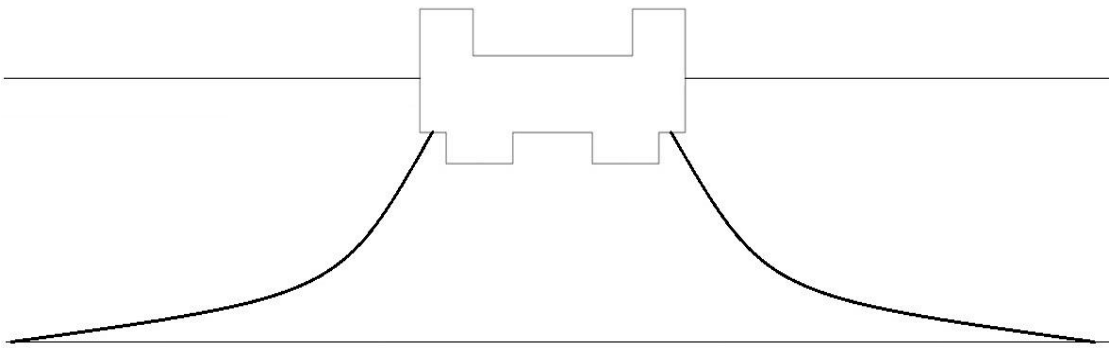

Figure 4.2: Catenary system (directional mooring)

4.3 EXPERIMENTAL RESULTS

Series of experiments were vigorously conducted in the wave tank to study the hydraulic performance on the H-Float in both regular waves and random waves. Some examples of raw data and the related wave analysis are demonstrated according to the

wave and mooring type in the following section. The experiments involved some variables that need to be tested which are type of waves (random and regular), type of mooring system (taut leg and catenary), wave periods and also wave heights. However, due to some limitation of the wave paddle, some tests which involved bigger value of wave height could not be carried out in the wave tank. A total of 84 tests were completed within the capability of the test facilities and apparatus. For each type of mooring systems, there are 42 tests that were conducted; 33 for regular and 9 for random waves.

Table 4.3: Value of wave heights and periods for both regular and random waves

	Wave Steepness, H/L		**0.04**	**0.05**	**0.06**
Type of Wave	**Wave period, T (s)**	**Frequency, f**	**Wave Height (m)**	**Wave Height (m)**	**Wave Height (m)**
Regular	0.8	1.25	0.04	0.05	0.06
	0.9	1.11	0.05	0.06	0.08
	1.0	1.00	0.06	0.08	0.09
	1.1	0.91	0.08	0.09	0.11
	1.2	0.83	0.09	0.11	0.13
	1.3	0.77	0.10	0.13	0.15
	1.4	0.71	0.11	0.14	0.17
	1.5	0.67	0.13	0.16	0.19
	1.6	0.63	0.14	0.17	0.21
	1.7	0.59	0.15	0.19	0.23
	1.8	0.56	0.16	0.20	0.25
Random	0.8	1.25	0.04	0.05	0.06
	1.0	1.0	0.06	0.08	0.09
	1.2	0.83	0.09	0.11	0.13

4.4 RESULTS INTERPRETATION

The wave energy coefficients C_t, C_r and C_l^2 are plotted against the breakwater width B/L where B and L are the breakwater width and the wavelength, respectively. The geometrical ratio of B/L is a well-accepted dimensionless parameter used in the design of coastal engineering structures. Since B is fixed in this study and the fact that L is the only independent variable that is governed by the change of wave period or

wave frequency, the *B/L* is often termed as the relative wave period or the relative wave length. Nevertheless, as far as this thesis is concerned, the *B/L* is consistently termed as the relative breakwater width throughout this writing.

4.4.1 Wave Transmission

In this experiment, wave transmission performance of the H-Float is quantified by the wave transmission coefficient, C_t. The lower the C_t values, the smaller the amount of wave transmission at the lee side of the breakwater which, in turn, leads to higher wave attenuation ability. If the transmission coefficient is small, then the breakwater is considered to be effective. It is because, the amount of energy that has transmitted past the floating structure is much less than the energy of incident wave.

4.4.1.1 Regular Wave

Figure 4.3 displays the C_t of the H-Float subjected to the type of mooring system in regular waves. The wave steepness tested ranges from 0.04 – 0.06.

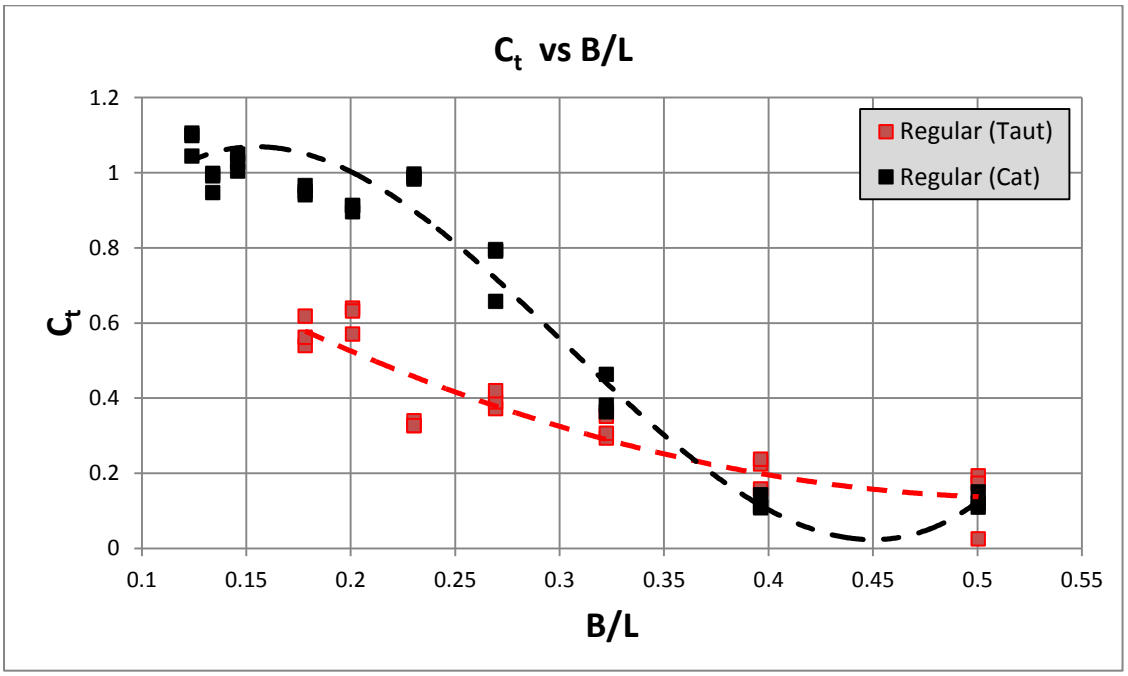

Figure 4.3: C_t vs. *B/L* of regular waves

Based on the figure above, it is found that the C_t recorded are relatively smaller ($C_t \leq 0.60$) for H-Float moored by taut leg system than the C_t recorded for H-

Float moored by catenary system ($C_t \leq 1.10$). This indicates that the taut leg system will give better wave attenuation compared to catenary. The C_t reduces as *B/L* increases from 0.18 to 0.50 and 0.13 to 0.50 for taut leg and catenary system respectively. The lowest C_t values recorded for taut leg system is 0.04 while for catenary system is 0.10, with both happen at *B/L* = 0.50. However, H-Float moored by catenary recorded the highest C_t value of 1.10. This means that the wave attenuation ability is not very effective for this type of mooring system.

The figure also demonstrate a decrease of C_t with an increase in *B/L*, indicating that the breakwater restricts wave transmission more effectively in seas dominated by shorter period waves. The summary of C_t for regular waves is presented in Table 4.4 below. In summary, the H-Float moored by taut leg can be regarded as a reasonably good wave attenuator, especially when adopted at sites exposed to shorter wave periods.

Table 4.4: C_t range for taut leg and catenary system (regular wave)

Mooring System	Taut Leg	Catenary
C_t Range	0.04 – 0.62	0.10 – 1.10
Average C_t	0.33	0.60

4.4.1.2 Random Wave

Figure 4.4 displays the C_t of the H-Float subjected to the type of mooring system in random waves. The wave steepness tested ranges from 0.04 – 0.06.

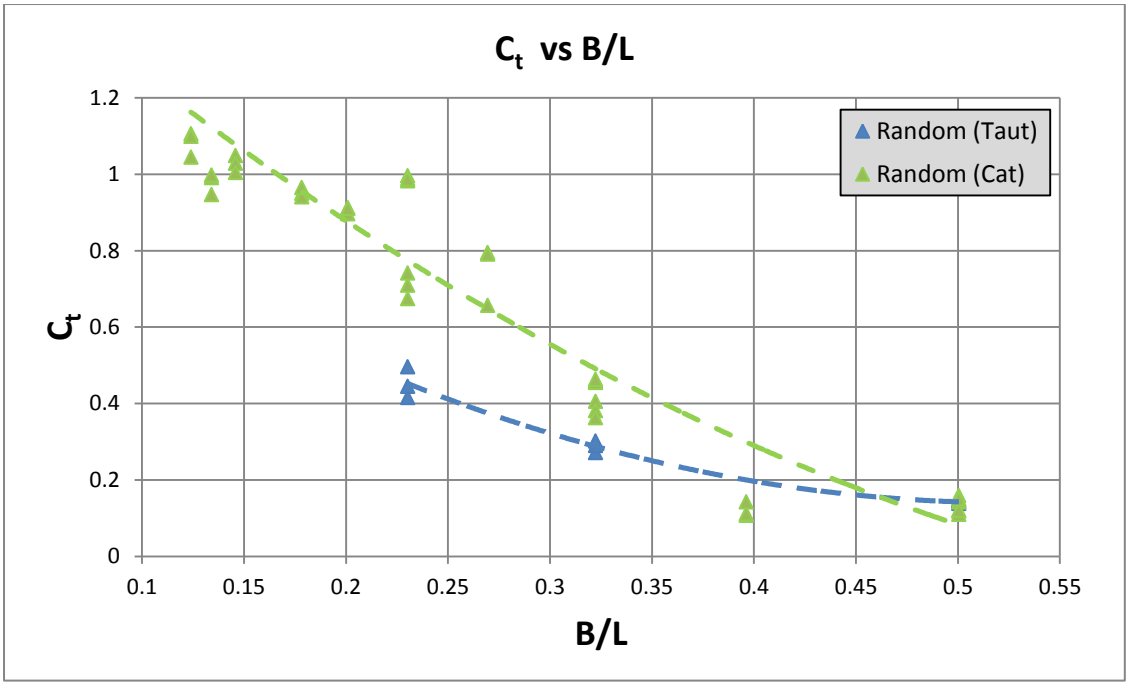

Figure 4.4: C_t vs. B/L of random waves

It is found that the C_t recorded are relatively smaller ($C_t \leq 0.50$) for H-Float moored by taut leg system than the C_t recorded for H-Float moored by catenary system ($C_t \leq 1.20$). This also indicates that the taut leg system will give better wave attenuation compared to catenary when the H-Float is tested with random waves. The C_t reduces as B/L increases from 0.23 to 0.50 and 0.13 to 0.50 for taut leg and catenary system respectively. There is no much different of C_t value recorded by regular and random wave for taut leg system. The lowest C_t values recorded for taut leg system is 0.12 while for catenary system is 0.10, with both happen at B/L = 0.50. However, H-Float moored by catenary recorded the highest C_t value of 1.10. This means that the wave attenuation ability in random wave is not very effective for this type of mooring system.

Same for regular wave, the figure also demonstrate a decrease of C_t with an increase in B/L, indicating that the breakwater restricts wave transmission more effectively in seas dominated by shorter period of random waves. The summary of C_t for regular waves is presented in Table 4.5 below. In summary, the H-Float moored by taut leg can be regarded as a reasonably good wave attenuator in random wave, especially when adopted at sites exposed to shorter wave periods.

Table 4.5: C_t range for taut leg and catenary system (random wave)

Mooring System	Taut Leg	Catenary
C_t Range	0.12 – 0.50	0.10 – 1.10
Average C_t	0.31	0.60

4.4.2 Wave Reflection

Wave reflection performance of the H-Float breakwater is quantified by the wave reflection coefficient, C_r. Reflection occurs when the waves hit on H-Float structure and are reflected back seaward. The lower the C_r values, the lesser will be the wave reflection effect. This means that low C_r values will give better results to that particular test.

4.4.2.1 Regular Wave

Figure 4.5 present the relationship between C_r and B/L of the H-Float subjected to the type of mooring system in regular wave. The wave steepness tested ranges from 0.04 – 0.06.

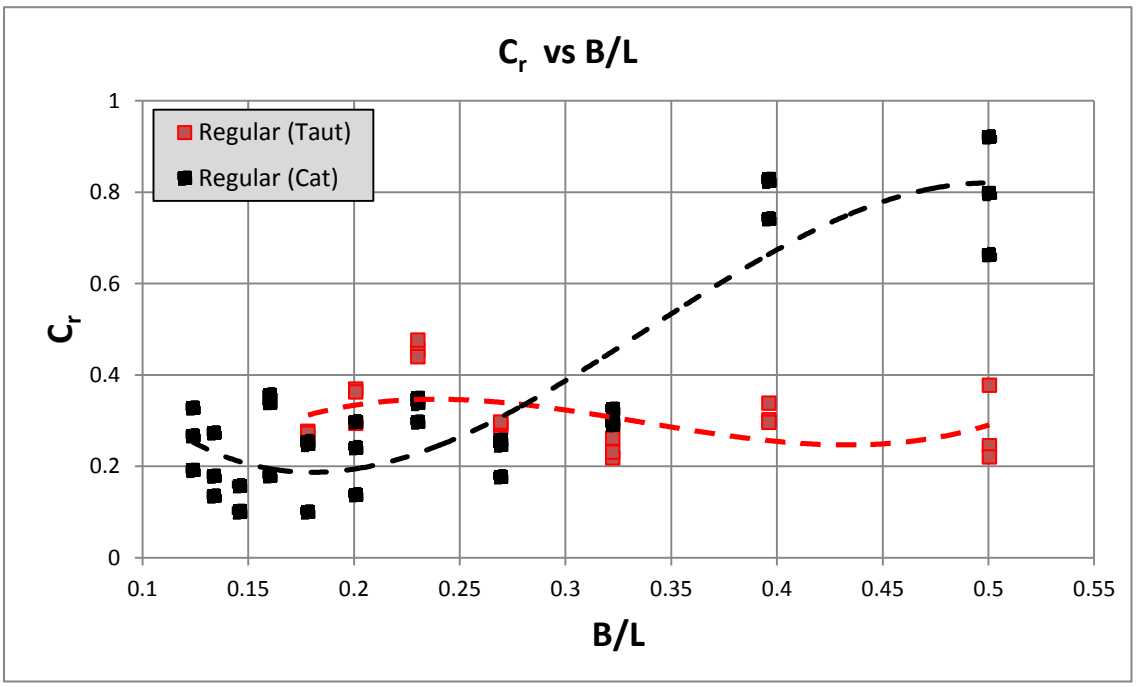

Figure 4.5: C_r vs. B/L of regular waves

From the figure above, the pattern of C_r values for taut leg system are quite steady in range between 0.22 - 0.45. Meanwhile, the C_r values for catenary system are strongly governed by the change of wave length (or wave period) as seen in the figure, i.e. the higher the *B/L*, the higher the C_r values. The lowest C_r recorded for taut leg system is at 0.22 while the highest is at 0.45. As *B/L* increases, it is surprising to notice that the C_r of catenary system strike the highest values of 0.92 and the lowest values of 0.10. This observation shows that the H-Float moored with catenary system could be a good reflection structure for shorter period.

However, H-Float moored with taut leg system is preferable because it reflect small wave back to the seaward which can be referred as good anti-reflection structure. The ranges of C_r for H-Float moored by taut leg and catenary system in regular waves are summarized in Table 4.6 below.

Table 4.6: C_r range for taut leg and catenary system (regular wave)

Mooring System	Taut Leg	Catenary
C_r Range	0.22 – 0.45	0.10 – 0.92
Average C_r	0.34	0.51

4.4.2.2 Random Wave

Figure 4.6 below present the relationship between C_r and *B/L* of the H-Float subjected to the type of mooring system in random wave. The wave steepness tested ranges from 0.04 – 0.06.

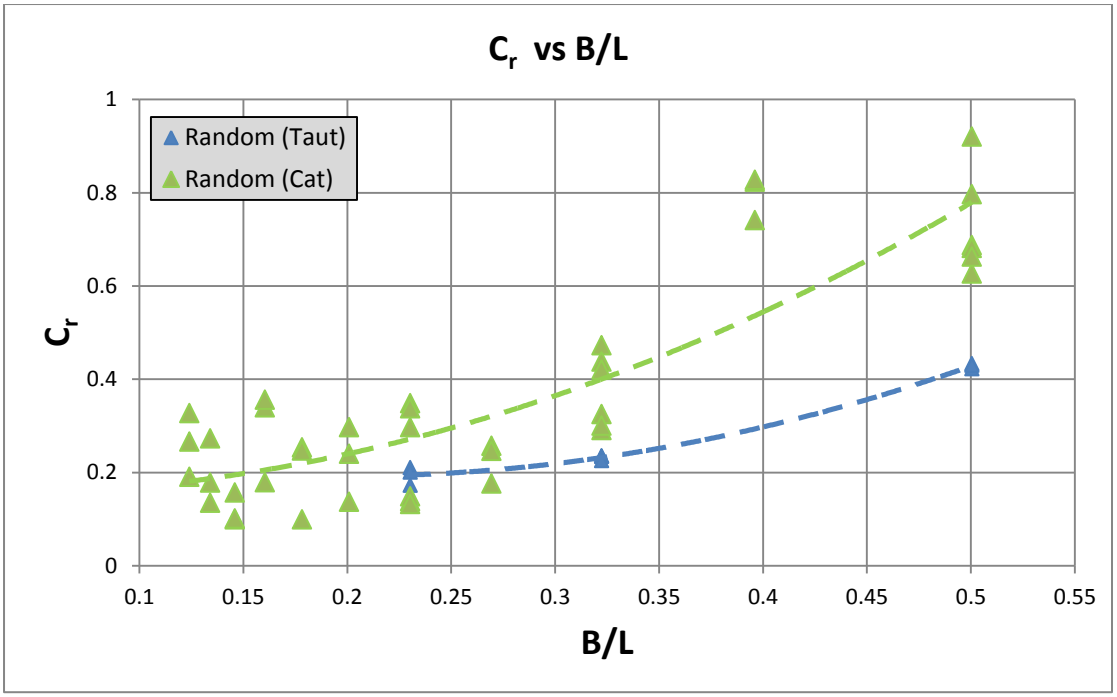

Figure 4.6: C_r vs. B/L of random waves

For random wave, the C_r values for both taut leg and catenary system increases as B/L increases. The lowest C_r value for taut leg system is 0.18 and the highest is 0.42. While the lowest C_r value for catenary system is 0.10 and the highest is 0.90. As expected, H-Float moored with taut leg provides the least C_r range than catenary system.

Questions may arise if the H-Float moored by taut leg is a good anti-reflection coastal structure. To answer the question, let's take at the highest C_r value attained by the breakwater based on the experimental results in this random wave. It is clear from the figure that the highest C_r recorded is about 0.42. This amount of reflected waves is relatively small as compared to the reflection caused by the bottom-mounted breakwaters, or even some of the floating breakwaters commercialized in the past decades.

The ranges of C_r for H-Float moored by taut leg and catenary system in regular waves are summarized in Table 4.7 below. In short, the H-Float moored with taut leg system is a good anti-reflection structure and is considered suitable to be adopted as wave defense structure at marinas and ports.

Table 4.7: C_r range for taut leg and catenary system (random wave)

Mooring System	Taut Leg	Catenary
C_r Range	0.18 – 0.42	0.10 – 0.90
Average C_r	0.30	0.50

4.4.3 Energy Dissipation

Wave energy dissipation of the H-Float is quantified by the energy loss/dissipation coefficient, C_l. The amount of energy loss due to the test model is reflected by the C_l^2 values. The higher the C_l^2 values, the greater will be the energy loss triggered by the H-Float. The mechanisms identified to trigger energy loss are wave breaking, wave run-up and run down, formation of eddies underneath the test model, sound and heat. Since these phenomena are difficult to be measured physically, the loss of energy is often quantified based on the Principle of Conservation of Energy which is presented in Section 2.3.

4.4.3.1 Regular Wave

Figure 4.7 present the C_l^2 of the H-Float plotted against *B/L*, subjected to taut leg and catenary system at moored in regular waves. The wave steepness tested ranges from 0.04 – 0.06.

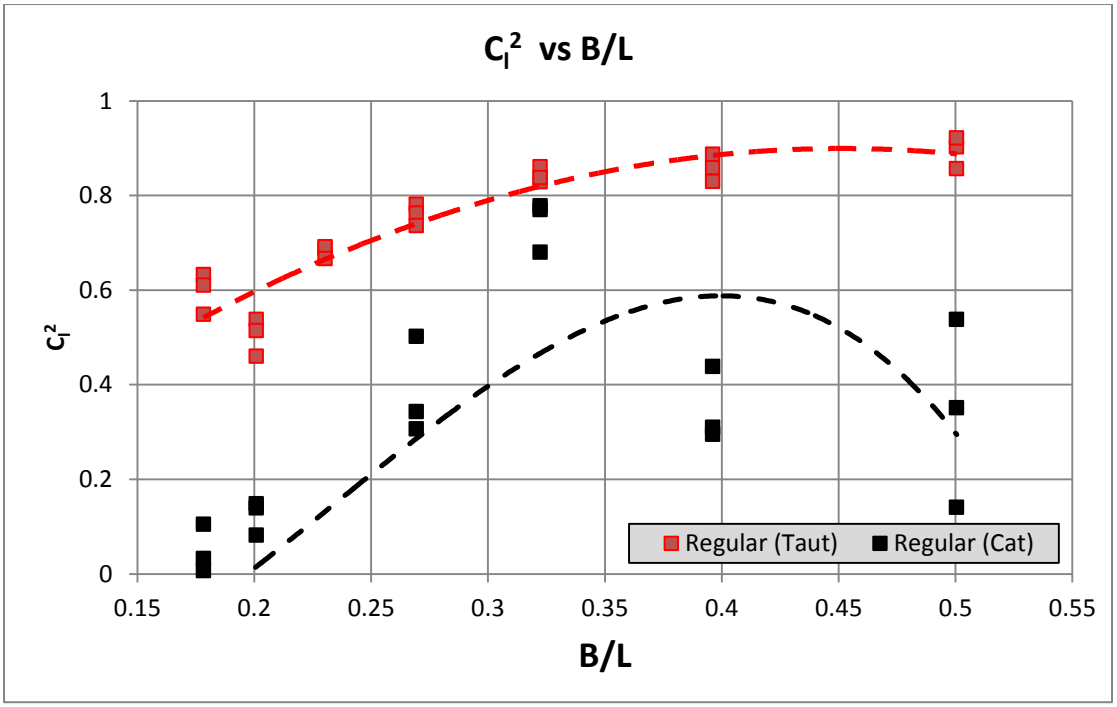

Figure 4.7: C_I^2 vs. B/L of regular waves

It is observed from the figure that the value of C_I^2 of H-Float moored by taut leg system is much higher than H-Float moored by catenary system. It can be seen also that the C_I^2 of the test models of different mooring systems alter much as B/L increases. This shows that the C_I^2 values are sensitive to the change of wave period. The lowest C_I^2 value recorded for taut leg system is 0.44 and the highest is 0.91. Meanwhile, H-Float moored with catenary system has the lowest C_I^2 value of 0.01 and the highest C_I^2 value of 0.53. From this observation, it shown that the H-Float moored by taut leg system is a good energy dissipater of different periods. The range and average values of C_I^2 are summarized in Table 4.8.

Table 4.8: C_I^2 range for taut leg and catenary system (regular wave)

Mooring System	Taut Leg	Catenary
C_I^2 Range	0.44 – 0.91	0.01 – 0.53
Average C_I^2	0.68	0.27

4.4.3.2 Random Wave

Figure 4.8 present the C_I^2 of the H-Float plotted against *B/L*, subjected to taut leg and catenary system at moored in random waves. The wave steepness tested ranges from 0.04 – 0.06.

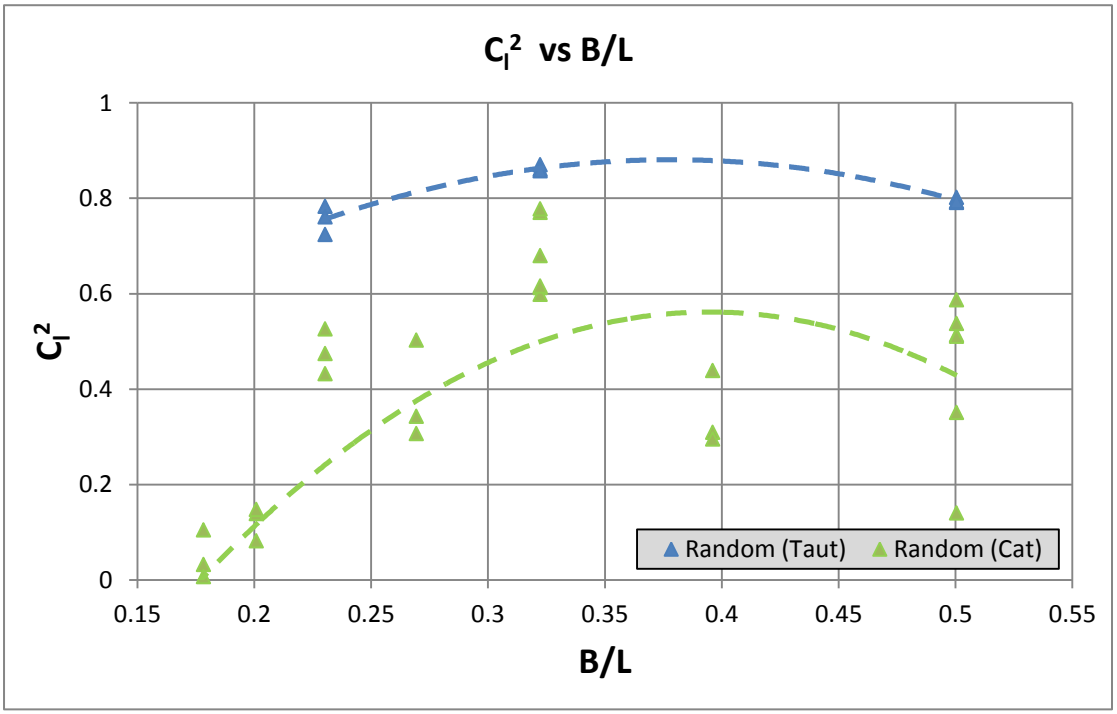

Figure 4.8: C_I^2 vs. *B/L* of random waves

Based on the figure, the results of C_I^2 for random wave is almost the same with the regular wave, where that the value of C_I^2 of H-Float moored by taut leg system is much higher than H-Float moored by catenary system. It is clearly seen that the C_I^2 of the test models of different mooring systems alter much as *B/L* increases and shows that the C_I^2 values are sensitive to the change of wave period. The lowest C_I^2 value recorded for taut leg system is 0.72 and the highest is 0.86. Meanwhile, H-Float moored with catenary system has the lowest C_I^2 value of 0.01 and the highest C_I^2 value of 0.78. From this observation, it proved that the H-Float moored by taut leg system is a good energy dissipater of different periods. The range and average values of C_I^2 are summarized in Table 4.9

Table 4.9: C_l^2 range for taut leg and catenary system (random wave)

Mooring System	Taut Leg	Catenary
C_l^2 Range	0.72 – 0.86	0.01 – 0.78
Average C_l^2	0.79	0.40

4.4.4 Effect of Wave Steepness Parameter

In this study, the wave energy coefficients of C_t, C_r and C_l^2 of the H-Float are also plotted with a dimensionless wave steepness parameter H_i/gT^2 where H_i is the incident significant wave height (equivalent to H_{m0}), g is the acceleration of gravity and T is the wave period. H_i/gT^2 is also one of the most commonly used parameters in the design of coastal structures. Since H_i always depends on the change of the variable T in this study, the H_i/gT^2 often termed as the relative wave steepness.

4.4.4.1 Wave Transmission

Figure 4.9 shows the relationship between C_t and H_i/gT^2 for both regular and random waves subjected to two types of mooring system which is taut leg and catenary. The C_t data for the respective waves and moorings spreads over the range of H_i/gT^2 with unnoticed variations. This proves that the wave attenuation performance of the H-type floating breakwater is less controlled by the steepness of waves. Nevertheless, it is seen from the figure that the C_T is more influenced by the types of mooring system.

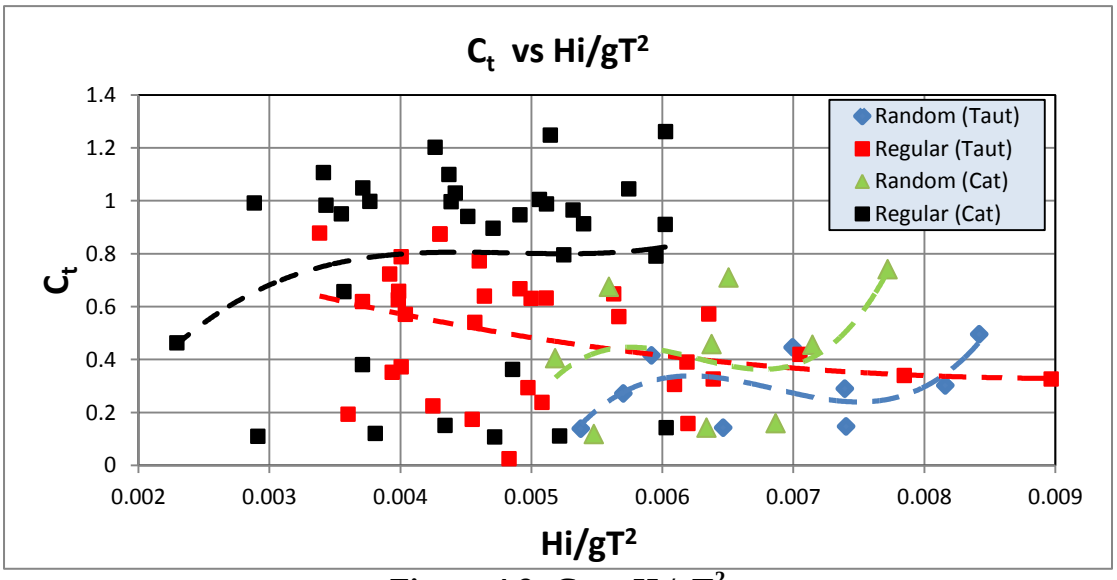

Figure 4.9: C_t vs H_i/gT^2

4.4.4.2 Wave Reflection

The response of C_r with respect to H_i/gT^2 is presented in Figure 4.10. The C_r data are rather scattered when plotted against H_i/gT^2 regardless of wave type or mooring system. The general behaviors of C_r are graphically represented by best-fit plots for the ease of interpretation of results. It is apparent that H_i/gT^2 may not be a significant design parameter to the reflective characteristics of the H-type floating breakwater.

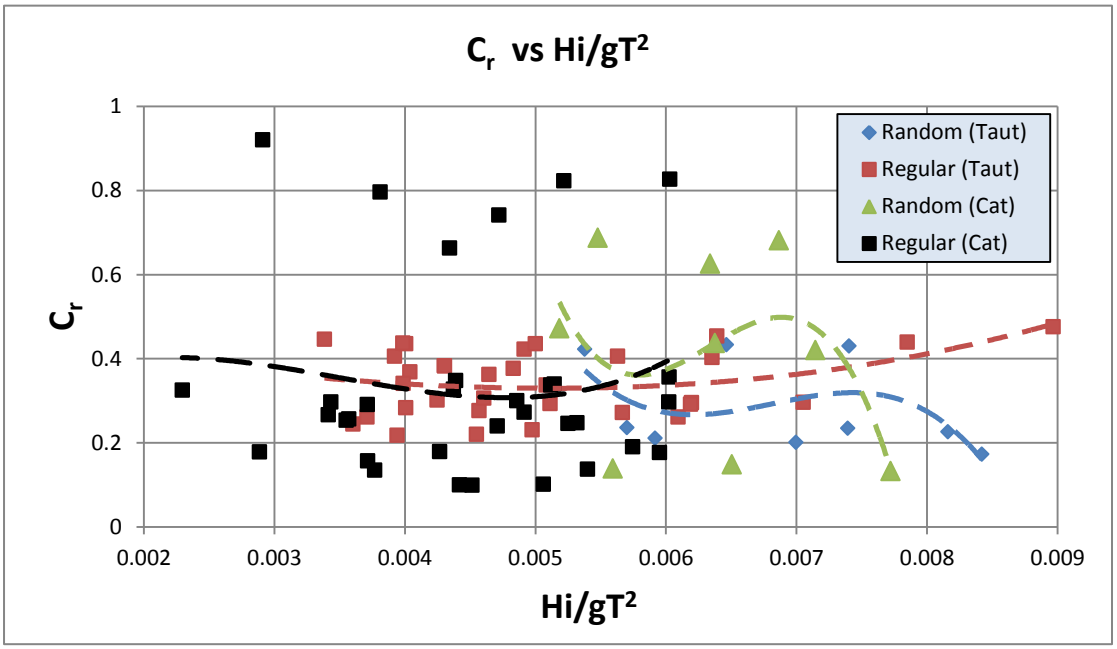

Figure 4.10: C_r vs H_i/gT^2

4.4.4.3 Energy Dissipation

The energy dissipation characteristic of the H-Float with respect to the relative wave steepness parameter is shown in Figure 4.11. It is apparent that the C_l^2 for both regular and random wave are closely related to each other. Similarly, H_i/gT^2 is not a governing parameter influencing C_l^2 within the tested type of mooring system. Hence, this parameter is suggested to be exempted when conducting the dimensional analysis for the energy coefficients of the H-Float.

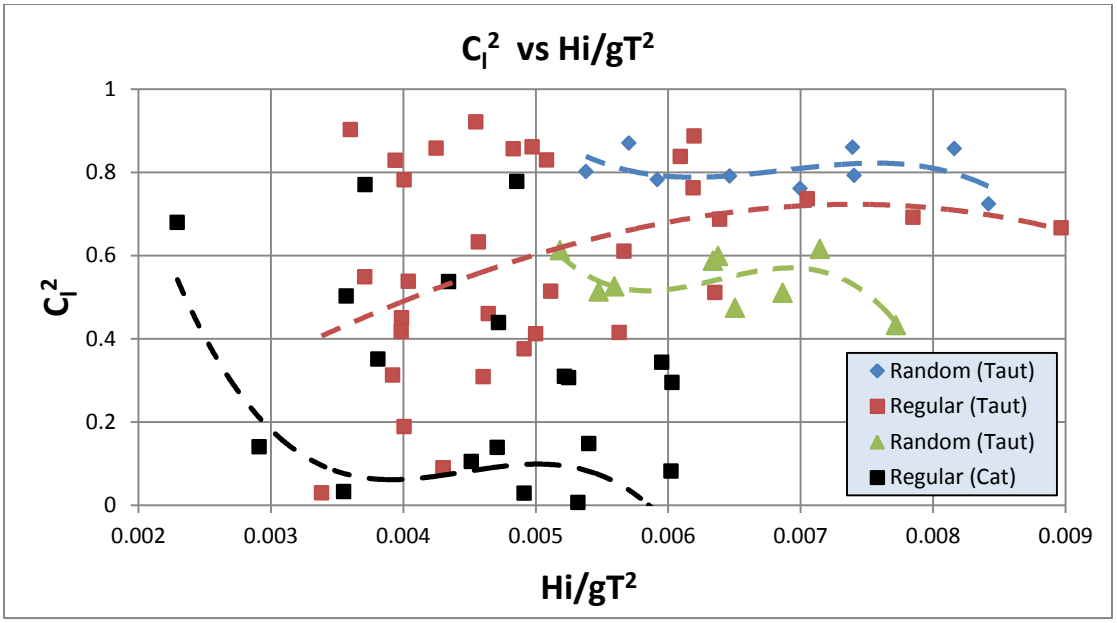

Figure 4.11: C_l^2 vs H_i/gT^2

4.5 COMPARISON OF RESULTS WITH OTHER FLOATING BREAKWATERS

The hydraulic performances of the H-Float is compared with those of other types of breakwater developed by other researchers, namely cage-type, pontoon-type, box-type, Y-frame type and other floating breakwaters as listed in Table 4.10. The comparison of C_t, C_r and C_l^2 are shown in Figures 4.11, 4.12 and 4.13 respectively. Note that these breakwaters were geometrically varied and were tested in different immersion depths and wave environments. Therefore, breakwater performance comparison can only be done qualitatively, and not quantitatively, in this study.

Reference	Structure type	Dimension of model [m]	Experimental facilities [flume/tank dimension & d in m]	Main parameters ranges	Hydrodynamics coefficients (C_t, C_r ,C_l)
Bruce L. McCartney (1985)	Box-type FBW (B = 12 FT)	B=4.0, l=29.7, h=1.5, D=1.1	Tested for Olympia Harbor, Washington, *d* = 7.6	H_i = 0.50-1.10, T=2.50-4.00	C_t = 0.42-0.88
Bruce L. McCartney (1985)	Box-type FBW (B = 16 FT)	B=4.8, l=29.7, h=1.5, D=1.1	Tested for Olympia Harbor, Washington, *d* = 7.6	H_i = 0.50-1.10, T=2.50-4.00	C_t = 0.39-0.89
Mani J.S. (1991)	Y-Frame FBW	B=0.5, l=0.2, 0.3, 0.4, h=0.3, D=0.16-0.46	30 x 2 x 1.5, *d* = 1.0	D/d =0.46, H_i/L = 0.01-0.10, B/L =0.095-0.224	C_t = 0.31-0.79
Murali K. and Mani J.S. (1997)	Cage FBW	B=0.6, 0.8, 1.0, l=0.2, 0.3, 0.4, h=0.3, D=0.36-0.56	30 x 2 x 1.5, *d* = 1.0	D/d=0.46, H_i/L = 0.01-0.10, B/L =0.12-0.60	C_t = 0.08-0.58
Behzad M. and Akbari M. (2007)	Moored Pontoon Type FBW	B=0.72, D=0.3-0.4	33 x 5.5 x 1.5, *d* = 1.0	D/d=0.14-0.23 H_i=0.20-1.20 B/L =0.20-2.20	C_t = 0.55-0.89
Wang H.Y. and Sun Z.C. (2010)	Porous FBW (Directional Mooring)	B=0.68, l=0.32, h=0.2, porosity=0.63,D=0.4-0.44	50 x 0.7 x 1.0, *d*=0.44	H_i = 0.06 T=0.60-1.40 B/L = 0.132-0.569	C_t = 0.10-0.94 C_r = 0.09-0.25 C_l = 0.40-0.99
Wang H.Y. and Sun Z.C. (2010)	Porous FBW (Directional Mooring)	B=0.68, l=0.32, h=0.2, porosity=0.63, D=0.4-0.42	50 x 0.7 x 1.0, *d*=0.44	H_i = 0.06 T=0.60-1.40 B/L = 0.132-0.569	C_t = 0.01-0.66 C_r = 0.09-0.28 C_l = 0.72-1.00
Fang He et al. (2012)	Rectangular FBW without pneumatic chambers	B=0.75, l=1.42, h=0.4, D=0.235	45 x 1.55 x 1.5, *d* = 0.7	H_i = 0.04 T=1.10-1.80 B/L = 0.186-0.404	C_t = 0.35-0.91 C_r = 0.39-0.55 C_l = 0.05-0.72
Fang He et al. (2012)	Rectangular FBW with pneumatic chambers	B=0.75, l=1.42, h=0.4, D=0.235	45 x 1.55 x 1.5, *d* = 0.45-0.90	H_i = 0.04 T=1.10-1.80 B/L = 0.187-0.430	C_t = 0.18-0.65 C_r = 0.15-0.72 C_l = 0.45-0.88
Teh H.M. and Nuzul I.M. (2012)	H-shape FBW	B=0.20, l=0.29, h=0.10, D=0.065	12 x 0.3 x 0.45, *d*=0.20-0.30	D/d=0.22-0.325 H_i/L = 0.025-0.125 B/L =0.10-0.50	C_t = 0.18-0.70
Nuzul I.M. (2012)	Improved H-shape FBW	B=0.20, l=0.30, h=0.10, D=0.05-0.103	10 x 0.3 x 0.45, *d*=0.20-0.30	D/d=0.17-0.52 H_i=0.005-0.075 B/L =0.10-0.50	C_t = 0.15-0.65
Dexter M. (2013)	H-type FBW 1:5	B=1.00, l=1.44, h=0.50, D=0.24-0.31	25 x 1.5 x 3.2, *d*=0.7	D/d=0.34-0.44 H_i/L = 0.04-0.07 B/L =0.22-0.65	C_t = 0.08-0.47 C_r = 0.73-0.87 C_l = 0.44-0.61
Mahadi N.N.A (2013)	H-type FBW 1:10	B=0.5, l=1.44, h=0.25, D=0.16	25 x 1.5 x 3.2, *d*=0.7	D/d=0.2286 H_i/L = 0.04-0.06 B/L =0.178-0.5	C_t = 0.29-0.57 C_r = 0.27-0.49 C_l = 0.58-0.68
Azmi M.S.S.M (2014)	H-Float 1:15	B=0.5, l=1.44, h=0.25, D=0.15	25 x 1.5 x 3.2, *d*=0.73	*D/d=0.205* *H_i/L=0.04-0.06* *B/L=0.13-0.50*	C_t = 0.12 – 0.50 C_r = 0.18 – 0.42 C_l = 0.44 – 0.91

Table 4.10: Characteristics of other floating breakwater models compared against H-Float in Figures 4.11 – 4.13

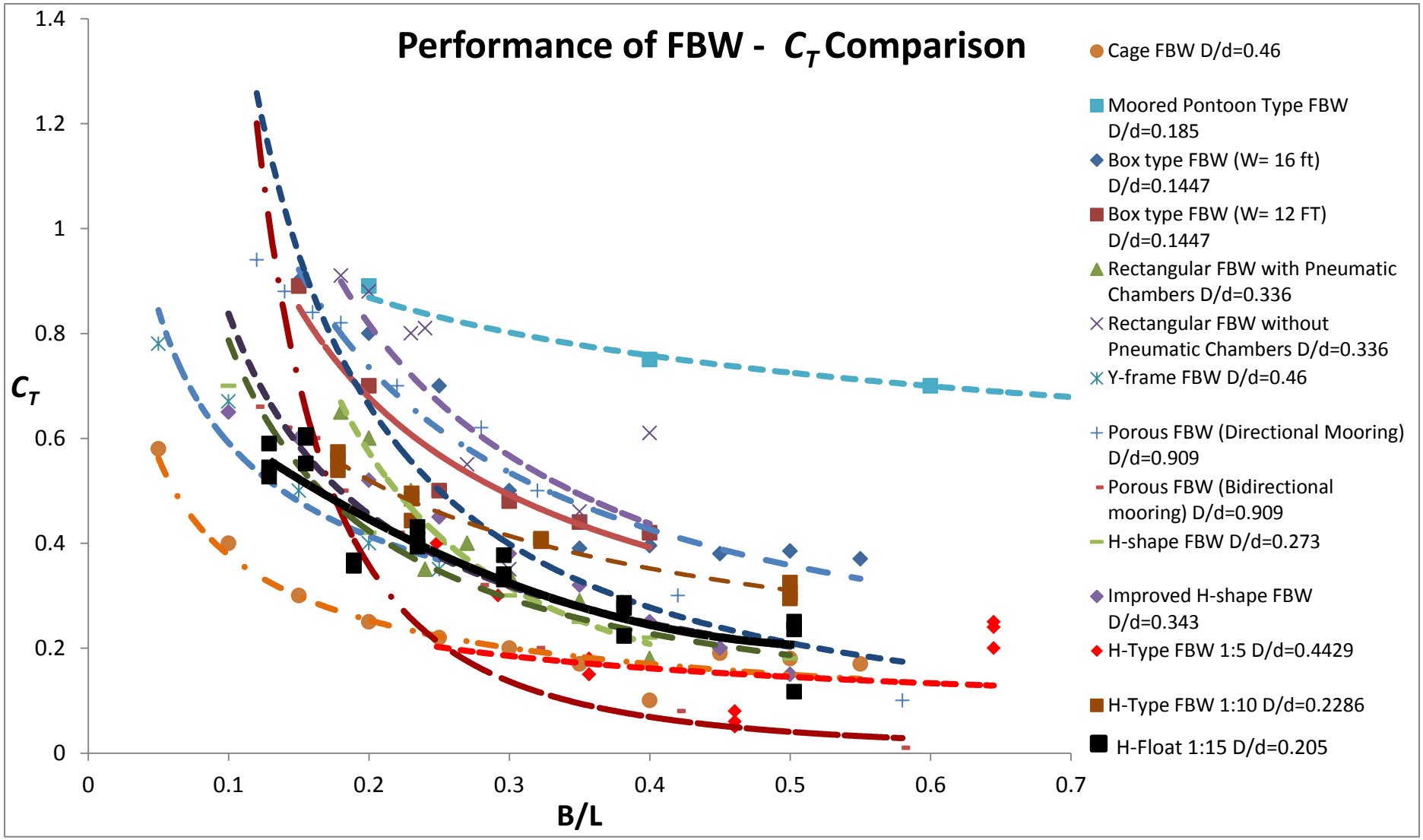

Figure 4.11: Comparison of transmission coefficient against other floating breakwaters

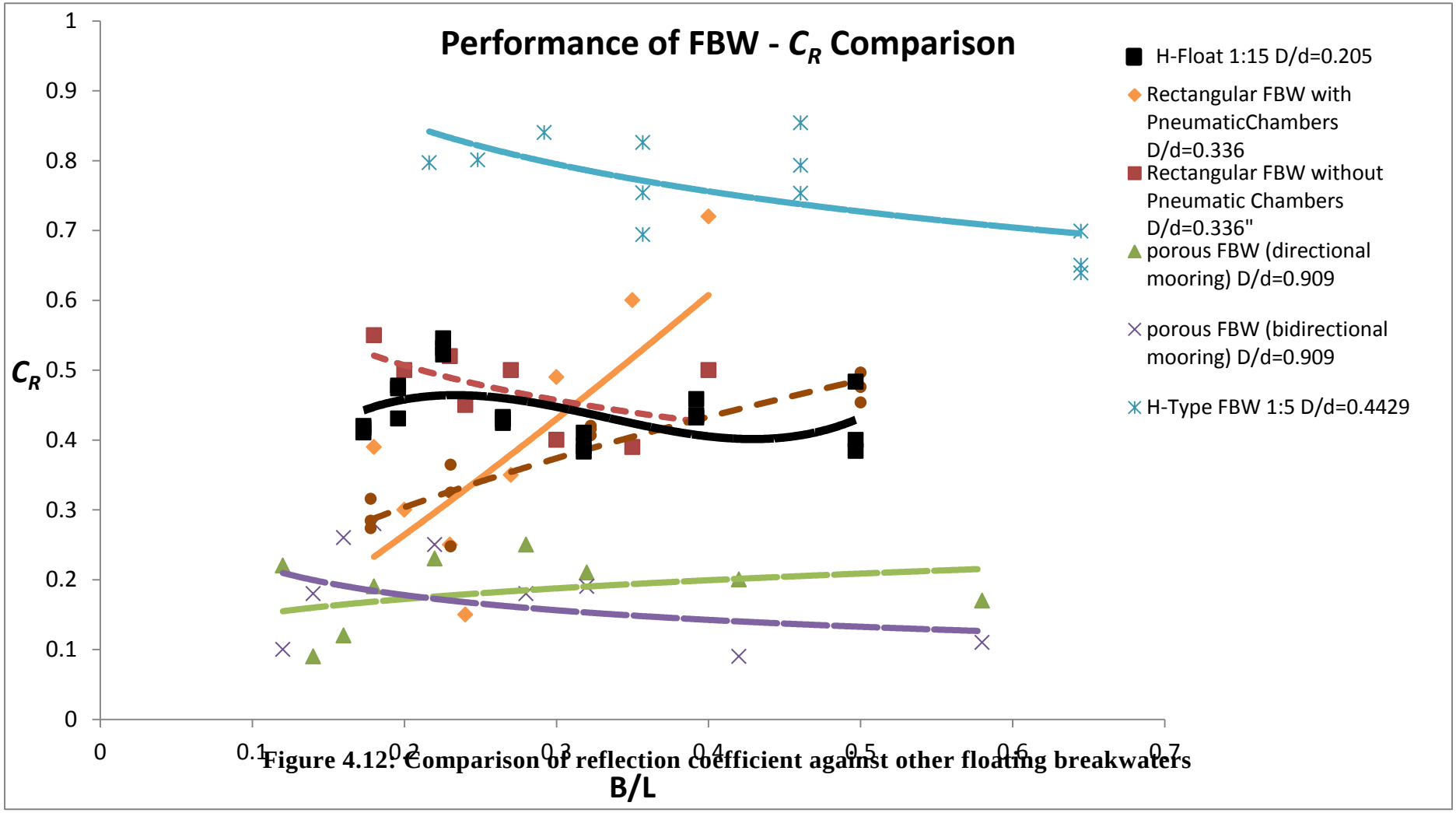

Figure 4.12: Comparison of reflection coefficient against other floating breakwaters

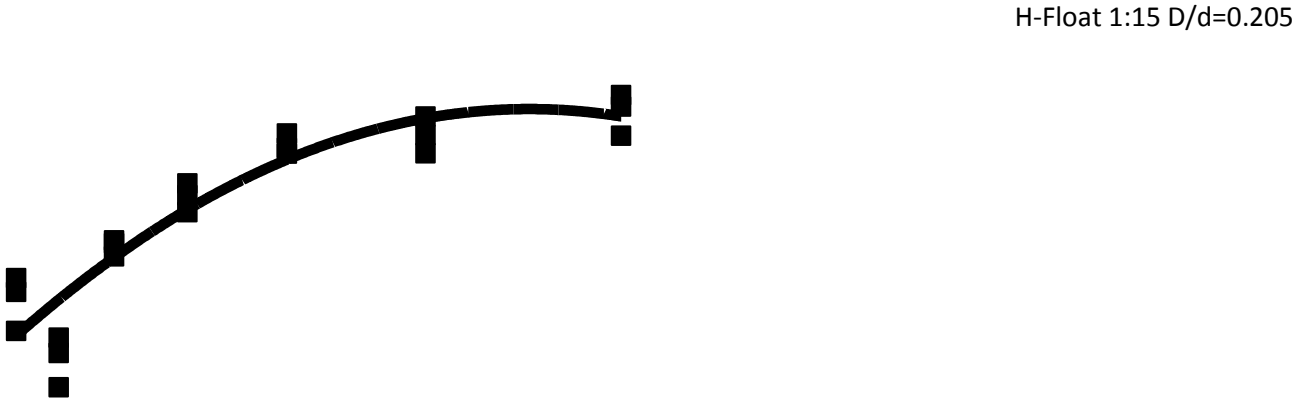

Figure 4.13: Comparison of energy dissipation against other floating breakwaters

Figure 4.11 shows the C_t of different types of floating breakwater corresponding to the relative breakwater width, *B/L*. The C_t of the H-Float seems to follow the trend of other breakwaters, i.e. smaller C_t in larger *B/L* range. The breakwaters that achieve low C_t (i.e. cage-type, porous-type, Y-frame type, etc) have deeper drafts with *D/d* ranges from 0.44 to 0.91. Based on the figure, it shows that the H-Float is a good wave attenuator compared with others as it has low transmission coefficient C_t with low *D/d* value. Thus, it proves that the draft of the floating breakwater is the key factor affecting the wave attenuation of the floating breakwaters of various configurations.

Besides, the reflectivity of the floating breakwater is presented in Figure 4.12. There is no definite trend in the C_r variation corresponding to *B/L* because the amount of wave reflection is considerably controlled by the geometrical aspect of the breakwater. Porous breakwater is a good anti-reflection structure because it permit the transmission of wave energy through the structure. However, it has quite high value of *D/d* as compared to other breakwaters. Thus, H-Float can be considered as the best anti-reflection structures as it has low value of reflection coefficient C_r with low value of *D/d.*

The energy dissipative performances of the floating breakwaters are shown in Figure 4.13. It is clear that the H-Float is an effective energy dissipater with lower *D/d* value. It is seen from the figure that the porous breakwater is highly energy dissipative due to its deep draft with porous medium. The box-type breakwater is less energy dissipative due to the fact that the structure is lack of sharp edges for promotion of flow separation and turbulence.

4.6 SUMMARY OF RESULTS

Table 4.11: Results' summary

Energy Coefficient	H-Float Moored by Taut Leg System		H-Float Moored by Catenary System	
	Regular	**Random**	**Regular**	**Random**
Wave Transmission (C_t)	LOW (0.18 – 0.42)	LOW (0.12 – 0.50)	HIGH (0.10 – 1.10)	HIGH (0.10 – 1.10)
Wave Reflection (C_r)	LOW (0.22 – 0.45)	LOW (0.18 – 0.42)	HIGH (0.10 – 0.92)	HIGH (0.10 – 0.90)
Energy Dissipation (C_l^2)	HIGH (0.44 – 0.91)	HIGH (0.72 – 0.86)	LOW (0.01 – 0.53)	LOW (0.01 – 0.78)

Based on the table above, it can be concluded that H-Float moored with taut leg system give better results as to compare with H-Float moored with catenary system, both for regular and random waves. It has lower transmission coefficient C_t, lower reflection coefficient C_r and higher energy dissipation coefficient C_l^2. H-Float moored with taut leg system is a good wave attenuator, good anti-reflection structure and also good energy dissipater.

CHAPTER 5

CONCLUSION AND RECOMMENDATION

5.1 CONCLUSIONS

A few major conclusions has been yielded based on the results of the analysis that has been conducted throughout the study of the performance of H-Float.

- Gain values are used as coefficients by wave generation program to generate specific wave height.

- Transmission coefficient analysis shows that the H-Float is a good wave attenuator. The coefficient decreases with increasing relative breakwater width and shorter wave length or *B/L* ratio. On top of that, the H-Float performed even better when it is moored with taut leg system rather than moored with catenary system.

- Reflection coefficient analysis indicates that more wave energy was being reflected by the model when the relative breakwater width increases or as the wavelength shortens when it is moored with taut leg system. It can be proved that H-Float is a good anti-reflection structure.

- Energy loss coefficient analysis reveals that the energy dissipation ability of the H-Float is sensitive to the changes in relative breakwater width or wave period as the value increases when B/L increases. H-Float moored with taut leg system gives higher value of reflection coefficient than moored with catenary system. It shows that the H-float is a good energy dissipater structure.

- Graphs of coefficients plotted against wave steepness parameter shows that the wave steepness has little to no effect on the overall attenuating ability of the breakwater.

- Comparison with previous studies indicates that the 1:15 H-Float model outperformed most breakwater models in term of wave attenuation, reflective measures and energy dissipation with regards of having the lowest breakwater

draft. The model can attenuate high wave energy when it is moored with taut leg system. The model also excels well in reflecting incident waves as less waves were reflected back to the seaward when compared to other floating breakwaters. The H-Float also was able to compete well in wave energy dissipation as it shows higher energy loss coefficient than other floating breakwaters model. It is deemed to be highly effective considering the small scale of model and breakwater draft as compared to the rest of breakwater models.

- The objective of the study was achieved as the model was tested in a condition that was similar to a typical sea condition.

- The performance of H-Float with scale of 1:15 is considered excellent and satisfactory. Further study with wider range of parameters will help in establishing the effectiveness of this breakwater design.

5.2 RECOMMENDATIONS

The H-type floating breakwater gave an overall satisfying performance in attenuating wave energy, both in regular and random waves. However, few recommendations are needed to further improve the performance and effectiveness of the H-Float as well as to avoid potential errors during the experiments.

- Further tests should include wider range of parameters with different values of relative breakwater width and varying water depth.
- The fabrication of model should focus on toughness of model to prepare the model for testing against larger waves with higher strength and energy.
- The integrity of equipment such as mooring lines and hooks should be strengthened to give higher durability.
- Installation of shock absorbance material on the sides of the model to prevent damage from collision against the wall of wave tank/flume.
- Further study on H-type breakwater model with focus on scale effects should be carried out to further validate the results of previous experiments.

REFERENCES

Bishop, C.T., 1982. Floating Tire Breakwater Comparison. *Journal of Waterway, Port, Coastal and Ocean Engineering*, 108(3), pp.421–426.

Brebner, A.O. A. Ofuya, 1968. Floating Breakwaters. *Proceeding of the 5th Coastal Engineering Conference*, pp.1055–1085.

Carver, D.D. R.D. Davidson, 1983. Sloping Float Breakwater Model Study. *Proceeding of coastal structure 83A speciality conference on design construction, maintenance and performance of coastal structure*, pp.417–432.

Chakrabarti, S. 1999. Wave interaction with an upright breakwater structure. *Ocean Engineering* 26, pp. 1003-1021.

Dong, G.H. Zheng, Y.N. Li, Y.C. Teng, B. Guan, C.T. Lin, D.F, 2008. Experiments on Wave Transmission Coefficients of Floating Breakwater. *Journal of Ocean Engineering*, 35, pp. 931-938.

Falcao, A., 2010. Wave Energy Utilization: A Review Of The Technologies. *Renewable sustainable energy*, 14(3), pp.899–918.

Hales, L.Z., 1981. *Floating Breakwater: State-of-the-art Literature Review, Technical Report No. 81-1*, U.S. Army, Corps of Engineers, Coastal Engineering Research Center.

He, A.W.-K. F. Huang Z. Law, 2013. An Experimental Study Of A Floating Breakwater With Asymetric Pneumatic Chambers For Wave Energy Extraction. *Journal of Applied Energy*, 106, pp.222–231.

Kato, Y. J. Hagino S. Uekita, 1966. Investigation Of Floating Breakwater To Which Anti-rolling System Is Applied. *Proceeding of the 10th Coastal Engineering Conference*, pp.1068–1078.

Kurum, M.O. 2010, *Box Type Floating Breakwaters,* Germany, Lambert Academic Publishing.

Mani, C.R. J.S. Venugopal, 1987. Wave Transmission Characteristics Of Floating Berrier. *Proceeding of 2nd national conference on docks and harbours engineering*, pp.53–59.

Mani, J., 1991. Design Of Y-frame Floating Breakwater. *Journal of Waterway, Port, Coastal and Ocean Engineering*, 117, pp.105–119.

McCartney, B.L., 1985. Floating Breakwater Design. *Journal of Waterway, Port, Coastal and Ocean Engineering*, 111, pp.304–317.

Murali, J.S. K. Mani, 1997. Performance Of Cage Floating Breakwater. *Journal of Waterway, Port, Coastal and Ocean Engineering*, pp.172–179.

Rahman, K. M.A. Mizutani N. Kawasaki, 2006. Numestudy Modeling Of Dynamic Responses And Mooring Forces Of Submerged Floating Breakwater. *Journal of Ocean Engineering*, 53, pp.799–815.

Shih, R.S, 2012. Experimental Study on the Performance Characteristics of Porous Perpendicular Pipe Breakwaters. *Journal of Ocean Engineering*, 50, pp. 53-62.

Tang, W.M. H.J. Hung C.C. Chen, 2011. Dynamics Of Dual Pontoon Floating Structure For Cage Aquaculture In A Two-dimensional Numerical Wave Tank. *Journal of Fluids and Structure*, 27, pp.918–936.

Teh, H.M. and Mohammed, N.I. 2012. Wave interactions with a floating breakwater. *Proceedings of the IEEE Colloquium on Humanities, Science and Engineering 2012.*

Wang, Z.C. H.Y. Sun, 2010. Experimental Study Of A Porous Floating Breakwater. *Journal of Ocean Engineering*, 37, pp.520–527.

Williams, A.G. A.N. Abul-Azm, 1997. Breakwaters Floating Breakwater. *Journal of Ocean Engineering*, 24, pp.465–478.

Yamamoto, T., 1981. Moored Floating Breakwater Response To Regular And Irregular Waves. *Journal of Applied Ocean Research*, 3(1), pp.114–123.

Vethamony, P., 1995. Wave Attenuation Characteristics of a Tethered Float system. *Journal of Ocean Engineering*, 22, pp.111–129.